CATCH OF THE NET

Biometrics refers to the identification of humans by their characteristics or traits. It is used for user identification and access control for computer systems security, secure electronic banking, secure access to buildings, and health and social services. It is also used to identify individuals in groups that are under surveillance. Biometric identifiers are distinctive and measurable characteristics that can be used to label and describe individuals, and can be categorised into physiological and behavioural characteristics. Physiological characteristics are related to the shape of the body, such as fingerprint, face, DNA, palm print, hand geometry, and iris and retina. Behavioural characteristics (known as behaviometrics) are related to the behaviour of a person, such as typing rhythm, handwriting, gait, and voice. As biometric identifiers are unique to individuals, they are more reliable in verifying identity than token and knowledge-based methods (such as driver's license and passport). While the costs of implementation biometric systems are high, the benefits of increased security and increase of accessibility by people of variable abilities can justify the costs. However, the collection of biometric identifiers raises privacy concerns about the ultimate use of this information. The following are relatively interesting and useful websites on biometrics:

1) **Biometrics.gov: Biometrics Overview**
   http://www.biometrics.gov/documents/biooverview.pdf

2) **Caslon Analytics: Biometrics**
   http://www.caslon.com.au/biometricsnote.htm

3) **How Stuff Works: How Biometrics Work**
   http://science.howstuffworks.com/biometrics.htm

4) **Bromba Biometrics: Biometrics FAQ**
   http://www.bromba.com/faq/biofaqe.htm

5) **A Survey of Biometric Recognition Methods**
   http://www.vcl.fer.hr/papers_pdf/A%20Survey%20of%20Biometric%20Recognition%20Methods.pdf

   Websites and articles discussing on the operations of various types of biometric systems.

6) **Fulcrum Biometrics: Glossary of Biometric Terms**
   http://climate.nasa.gov

   Provides definitions for key biometric terms based on information derived from the US National Science & Technology Council (NSTC) Subcommittee on Biometrics.

7) **Federal Bureau of Investigation's (FBI) Biometric Center Of Excellence (BCOE)**
   http://www.biometriccoe.gov

   BCOE is the FBI's programme for exploring and advancing the use of new and enhanced biometric technologies and capabilities for integration into law enforcement operations.

8) **University of Bologna: Biometric System Laboratory**
   http://biolab.csr.unibo.it/home.asp

9) **Carnegie Mellon University: Cylab Biometric Center**
   http://www.cylab.cmu.edu/research/center-biometrics.html

10) **Michigan State University: Biometrics Research Group**
   http://biometrics.cse.msu.edu

11) **Multimedia University: Centre for Information Security (CIS)**
   http://fist.mmu.edu.my/cis

   Research centres focussed on emerging biometric technologies.

DEFENCE S&T TECHNICAL BULLETIN

Vol. 6 | Num. 2 | Year 2013 | ISSN 1985-6571

CONTENTS

STRIDE™ SCIENCE & TECHNOLOGY RESEARCH INSTITUTE FOR DEFENCE

ISSN 1985-6571

AIMS AND SCOPE

The Defence S&T Technical Bulletin is the official technical bulletin of the Science & Technology Research Institute for Defence (STRIDE). The bulletin, which is indexed in, among others, Scopus, Index Corpenicus, ProQuest and EBSCO, contains manuscripts on research findings in various fields of defence science & technology. The primary purpose of this bulletin is to act as a channel for the publication of defence-based research work undertaken by researchers both within and outside the country.

WRITING FOR THE DEFENCE S&T TECHNICAL BULLETIN

Contributions to the bulletin should be based on original research in areas related to defence science & technology. All contributions should be in English.

PUBLICATION

The editors' decision with regard to publication of any item is final. A manusript is accepted on the understanding that it is an original piece of work which has not been accepted for publication elsewhere. Contributors will receive two complimentary copies of the issue in which their work appears.

PRESENTATION OF MANUSCRIPTS

The format of the manuscript is as follows:

a) Page size B5 (JIS)
b) MS Word format
c) Single space
d) Justified
e) In Times New Roman ,11-point font
f) Should not exceed 20 pages, including references
g) Texts in charts and tables should be in 10-point font.

Please e-mail the manuscript to:

1) Dr. Zalini bt Yunus (zalini.yunus@stride.gov.my)
2) Dr. Mahdi bin Che Isa (mahdi.cheisa@stride.gov.my)
3) Dr. Dinesh Sathyamoorthy (dinesh.sathyamoorthy@stride.gov.my)

The next edition of the bulletin is expected to be published in April 2014. The due date for submissions is 19 February 2014. **It is strongly iterated that authors are solely responsible for taking the necessary steps to ensure that the submitted manuscripts do not contain confidential or sensitive material.**

The template of the manuscript is as follows:

TITLE OF MANUSCRIPT

Name(s) of author(s)

Affiliation(s)

E-mail:

ABSTRACT

Contents of abstract.

Keywords: *Keyword 1; keyword 2; keyword 3; keyword 4; keyword 5.*

1. TOPIC 1

Paragraph 1.

Paragraph 2.

1.1 Sub Topic 1

Paragraph 1.

Paragraph 2.

2. TOPIC 2

Paragraph 1.

Paragraph 2.

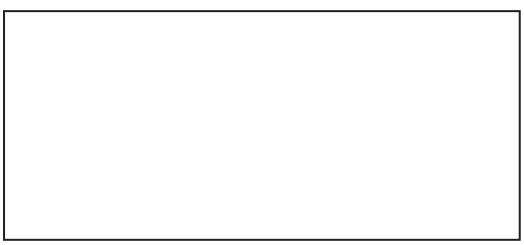

Figure 1: Title of figure.

Table 1: Title of table.

Content	**Content**	**Content**
Content	Content	Content
Content	Content	Content
Content	Content	Content

Equation 1 (1)
Equation 2 (2)

REFERENCES

Long lists of notes of bibliographical references are generally not required. The method of citing references in the text is 'name date' style, e.g. 'Hanis (1993) claimed that...', or '…including the lack of interoperability (Bohara *et al.*, 2003)'. End references should be in alphabetical order. The following reference style is to be adhered to:

<ins>Books</ins>

Serra, J. (1982). *Image Analysis and Mathematical Morphology*. Academic Press, London.

<ins>Book Chapters</ins>

Goodchild, M.F. & Quattrochi, D.A. (1997). Scale, multiscaling, remote sensing and GIS. *In* Quattrochi, D.A. and Goodchild, M.F. (Eds.), *Scale in Remote Sensing and GIS*. Lewis Publishers, Boca Raton, Florida, pp. 1-11.

<ins>Journals / Serials</ins>

Jang, B.K. & Chin, R.T. (1990). Analysis of thinning algorithms using mathematical morphology. *IEEE T. Pattern Anal.*, **12**: 541-550.

<ins>Online Sources</ins>

GTOPO30 (1996). *GTOPO30: Global 30 Arc Second Elevation Data Set*. Available online at: http://edcwww.cr.usgs.gov/landdaac/gtopo30/gtopo30.html (Last access date: 1 June 2009)

<ins>Unpublished Materials (e.g. theses, reports and documents)</ins>

Wood, J. (1996). *The Geomorphological Characterization of Digital Elevation Models*. PhD Thesis, Department of Geography, University of Leicester, Leicester.

Defence S&T Tech. Bull., 6(2): 78-92, 2013

ELECTROCHEMICAL CHARACTERISATION OF HYBRID ACTIVATORS FOR ALUMINIUM SACRIFICIAL ANODES IN NATURAL SEA WATER

Mohd Subhi Din Yati[1*], Mohd Nazree Derman[1], Mahdi Che Isa[2]
Mohd Moesli Mohammad[2] & Hasril Nain[2]

[1]School of Materials Engineering, University Malaysia Perlis (UniMap), Malaysia
[2]Materials Research Group, Maritime Technology Division, Science & Technology Research Institute for Defence (STRIDE), Malaysia

[*]E-mail: mohdsubhidinyati@yahoo.com

ABSTRACT

This paper reports on the electrochemical behaviour of as-cast Al-Zn-Mg alloys activated by tin (Sn) and ruthenium dioxide (RuO_2) in natural sea water. The potential and advantages of Sn and RuO_2 as hybrid activators in Al-Zn-Mg alloys will be studied by using direct (DC) and alternating (AC) current electrochemical measurement techniques. The morphology of the alloys' corroded surface was studied using a scanning electron microscope (SEM). This study showed that the addition of 1.5%wt. Sn as an alloying element gave a stable corrosion free process that can be achieved after 2 ks of immersion. The results also showed that RuO_2 catalytic coating applied on the surface of Al-Zn-Mg-Sn alloy slightly shifted the values of open circuit potential (OCP) towards a more electropositive direction as compared to Al-Zn-Mg-Sn without RuO_2. The morphology of the corroded surface of Al-Zn-Mg-Sn alloy coated with RuO_2 showed a more uniform corrosion attack with the formation of porous and fibrous mud-like cracks on the outer layer. This type of corrosion morphology features were believed to facilitate ionic species adsorption and diffusion through corrosion product layer at solution-alloy interface. Electrochemical impedance spectroscopy (EIS) showed that both Sn and RuO_2 are capable to activate Al-Zn-Mg-Sn alloy in sea water by modifying the electrical properties of the oxide layer, reducing resistance to polarisation R_p values and thus, activating and accelerating the aluminium alloy dissolution process.

Keywords: *Aluminium sacrificial anodes; hybrid activators; electrochemical impedance spectroscopy (EIS); open circuit potential (OCP); corrosion morphology.*

1. INTRODUCTION

Sacrificial anode for cathodic protection (SACP) is one of the popular electrochemical means for corrosion mitigation in marine environments. The application of aluminium sacrificial anodes for the cathodic protection of steel structures has been practiced since the early 1960s (Barbucci *et al.*, 1997; Shibli *et al.*, 2005; Andrea *et al.*, 2011). Aluminium (Al) is generally used in ports to protect structures (e.g., docks and piles) because of its higher theoretical efficiency (Qingfeng & Niels, 2002; Jingling & Jiuba, 2010; Jiuba *et al.*, 2011; Junguang *et al.*, 2011) and its merits, such as low density, vast availability, reasonable cost (Shibli *et al.*, 2008) and the capability to provide enough driving potential throughout its service life as compared to zinc sacrificial anodes (Qingfeng & Neils, 2002). The first practical use of catholic protection was proposed by Sir Humprey Davy in 1820 for the Royal Navy in preserving copper sheeting used for cladding the hulls of naval vessels with small quantities of iron or zinc. Towards the end of the 1990s, when marine engineers realised that stern drives and outboard motors required more protection than zinc anodes could provide, suitable candidates, such as aluminium anodes, started to be used widely because of their much higher current capacity (Ah/kg) (Idusuyi & Oluwole, 2012). Sacrificial anodes have a difficult task, since they have to protect what is already a very active aluminium assembly. Installing cheap or sub-standard anodes also will undoubtedly cause increased and potentially very expensive corrosion problems.

Problems such as long periods of potential stabilisation, domination of pitting aided dissolution and surface passivation are common for aluminium sacrificial anodes. Aluminium also has a natural tendency of forming a passive oxide layer, but this can be overcome by the addition of alloying elements (Umoru & Ige, 2007; Mahdi *et al.* 2010, 2011) and catalytic coating (Shibli & Gireesh, 2003; Shibli *et al.*, 2004; Shibli & Gireesh, 2005; Shibli & Sony, 2007). Both methods are meant to generate surface modification, such as micro-structural electronic defects, that may lead to passive oxide film rupture. The alloying elements and catalytic coating will disturb the alumina (Al_2O_3) bonding strength by placing impurities in between the oxide-substrate layer (Jafarzadeh *et al.*, 2008). The addition of alloying elements such as mercury (Hg), gallium (Ga), indium (In), tin (Sn) and bismuth (Bi) (Shibli & Gireesh, 2003; Bessone, 2006) may weaken the oxide layer by easing ion penetration from electrolytes through the defective oxide layer, thus generating localised corrosion, which is also known as pitting corrosion. Hybrid activators, such as iridium dioxide (IrO_2) and ruthenium dioxide (RuO_2), have been extensively used as catalytic coating for chlor-alkali production and dimensionally stable anodes (DSAs) due to it good catalytic activity (Shibli & Sony, 2007; Likun *et al.*, 2009).

This paper will report on the electrochemical behaviour of as-cast Al- Zn-Mg alloys activated by Sn and RuO_2, because of their good characteristics in natural sea water (Mahdi *et al*, 2010; Shibli *et al.*, 2004). The potential and advantages of Sn and RuO_2 as hybrid activators in Al-Zn-Mg alloys will be studied by using direct (DC) and alternating (AC) current electrochemical measurement techniques.

2. MATERIALS & METHODS

2.1 Sample Preparation and Alloy Composition

Cast aluminium alloy was prepared in a graphite crucible under the protection of argon gas (inert atmosphere). Pure metals were melted in the crucible at temperature of 850 ^oC using aluminium beads (purity of 99.90%) as the primary component. Rod shaped samples were made using a preheated mild steel mould. As for the Al-Zn-Mg-Sn alloy fabrication, 1.5%wt Sn was added into an aluminium melted solution when approaching 650 ^oC to minimise Sn oxidation. At the same time, argon gas was flowed into the surrounding chamber at increased rate from 5 to 8 L/min. The sample was then cooled down at room temperature. The as-cast aluminium was then cut using a low speed cutter at speed of 250 rpm. The samples were then polished using 400, 600, 800 and 1,000 grades emery paper for the final surface preparation. The samples were degreased and washed using acetone and distilled water. In order to obtain an aluminium alloy coated with RuO_2, the samples were then dipped in 1,000 ppm $RuCl_3$ solution, and then dried and heated at 400 ^oC for 30 min. The composition of the prepared aluminium alloy samples are shown in Table 1.

Table 1: Aluminium alloy chemical compositions analysed using a wavelength dispersive x-ray fluorescent (WDXRF) spectrometer.

Sample	Code	Composition (wt %)					
		Zn	Mg	Sn	Fe	Pb	Al
Al-Zn-Mg	A	5.39	1.96	-	0.051	0.004	Bal.
Al-Zn-Mg-Sn	B	5.38	1.87	1.42	0.013	0.0007	Bal.
Al-Zn-Mg-Sn coated with 1,000ppm RuO_2	C	5.42	1.86	1.42	0.044	0.006	Bal.

2.2 Electrochemical Measurement

Open circuit potential (OCP), electrochemical impedance spectroscopy (EIS) and potentiodynamic polarisation measurement were conducted using a three-electrochemical cell GAMRY Instruments Reference 3000 potentiostat/galvanostat/zero resistance ammeter (ZRA) controlled by GAMRY Framework V5.65, and the Echem Analyst software for data analysis. A saturated calomel electrode (SCE) was used as the reference electrode (RE), while high density graphite was used as the counter electrode (CE). The sample was cut from the as-cast cylindrical alloy and drilled. The samples (5 mm thick) were then polished up to grit 1,000 followed by ultrasonic cleaning and finally dried in warm flowing air prior to each experiment. Potentiodynamic polarisation measurement was started from cathodic potential of -250 mV and stopped at anodic potential of 1,600 mV, with the scanning rate set at 0.5 mA/sec. Each sample's exposed area was 2.54 cm^2, embedded in cold mount resin with the copper wire stage-out for ease of electrical contact later in the experimental process. The experiments were conducted in sea water (natural chloride solution) at 27 ^oC (room temperature) and pH 8.1 with chemical composition as shown in Table 2. The sea water was taken from Teluk Batik, Perak, which is located at the west coast of Peninsular Malaysia. Impedance spectra were generated for the OCP values of the samples over frequency range of 100 kHz to 0.01 Hz. An AC signal of 0.5 mV was used in this impedance measurement.

Table 2: Natural sea water composition at room temperature (27 °C).

Cation (mg/l)		Anion (mg/l)		Trace elements (mg/l)	
(i) Natrium	9.247×10^3	(i) Chloride	15.451×10^3	(i) Barium	43.945×10^{-3}
(ii) Calcium	3.647×10^2	(ii) Sulphate	5.786×10^3	(ii) Manganese	38.451×10^{-3}
(iii) Magnesium	1.117×10^3	(iii) Fluoride	4.85×10^2	(iii) Copper	<0.001
(iv) Kalium	3.557×10^2	(iv) Nitrate	6.34×10^2	(iv) Zinc	0.122
(v) Boron	5.13×10^2	(v) Bromide	-	(v) Argentum	291.222×10^{-3}
(vi) Strontium	7.009			(iv) Plumbum	<0.001
				(vi) Cadmium	<0.001
				(vii) Chromium	<0.001
				(viii) Nickel	0.002
				(ix) Mercury	0.003
				(x) Arsenic	0.001

3. RESULTS AND DISCUSSION

3.1 Open Circuit Potential (OCP)

OCP measurement was recorded in sea water for a period of 15 h. As observed in Figure 1, Al-Zn-Mg-Sn (c) and Al-Zn-Mg-Sn coated RuO_2 (d) only took 2.5 ks of immersion to reach a stable free corroding potential. However, for Al-Zn-Mg, a stable OCP was achieved at approximately 45 ks of immersion time. From the OCP plots, it is concluded that the addition of Sn had a very important role in stabilising the OCP readings and shortening the time of activation, which is consistent with the findings in Mahdi *et al.* (2010). This finding is also in good agreement with studies conducted by previous researchers which reported on the role of Sn in activating magnesium anodes for battery applications (Feng *et al.*, 2007; Feng *et al.*, 2008).

For Al-Zn-Mg-Sn coated with RuO_2, the OCP plot shifts towards an electropositive direction as compared to Al-Zn-Mg-Sn. This is probably due to poor RuO_2 crystallites formation and a high electrical resistivity layer impeding the ionic movement. Both situations can be overcome using an annealing process as suggested by Shibli *et al.* (2004). The OCP values for the steel and aluminium alloy samples used in the experiment are shown in Table 3.

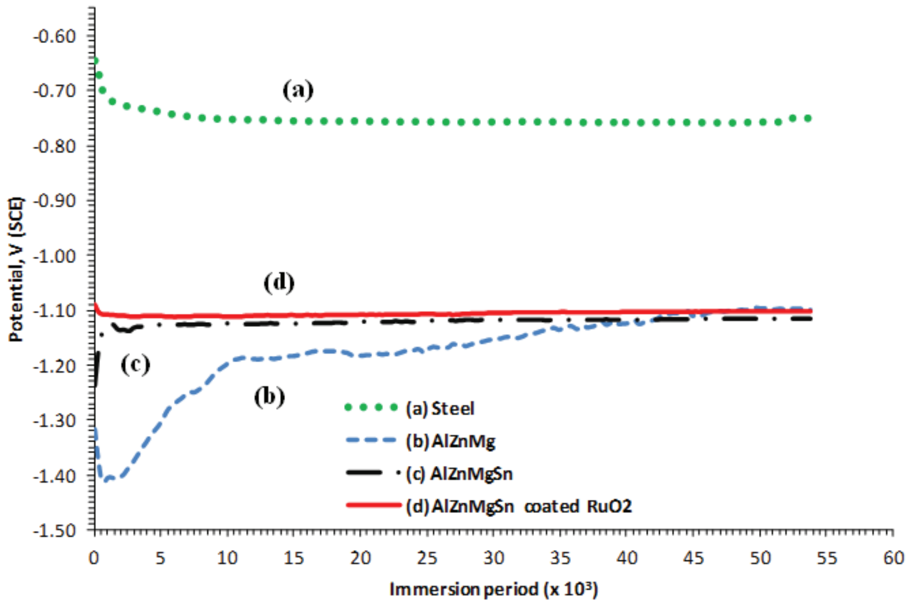

Figure 1: OCP values as a function of immersion time in sea water for aluminium alloys compared to steel.

Table 3: OCP values of the samples.

Alloys	OCP (mV vs SCE)
Al-Zn-Mg	-1096 ± 11
Al-Zn-Mg-Sn	-1152 ± 9
Al-Zn-Mg-Sn coated RuO_2	-1104 ± 9
Steel	-741 ± 7

The corrosion attack morphologies for the Al-Zn-Mg, Al-Zn-Mg-Sn and Al-Zn-Mg-Sn coated RuO_2 samples are shown in Figure 2. Localised corrosion attack was observed for the Al-Zn-Mg sample (b) due to the active nature of Mg as compared to Zn and Al matrix (Mahdi *et al.*, 2011). On the other hand, for the Al-Zn-Mg-Sn (b) and Al-Zn-Mg-Sn coated RuO_2 (c) samples, the attacks look more uniform. The morphologies of corrosion products formed after 10 h of immersion is a mud-crack morphology, reported by (Shibli & Gireesh, 2003; Shibli *et al.*, 2007). Severe corrosion attacks can be seen in Figures 2(b) and (c), which show that more surface disintegration occurs, which can be anticipated from the high surface uniformity in the Al-Zn-Mg-Sn sample based on the OCP plot.

Less severe corrosion attack was observed from the Al-Zn-Mg sample because of the limited surface activation at the alloy-solution interface. According to Orozco *et al.* (2007), the activation of Al-Zn-Mg alloy depends on the formation and dissolution of the intermetallic phase presence in the alloy. If the distribution of intermetallic or secondary phase is localised, corrosion attack will take place locally and will facilitate larger particles to disintegrate from the main material, which is known as the chunk effect. This phenomenon will in turn reduce the current capacity of the material.

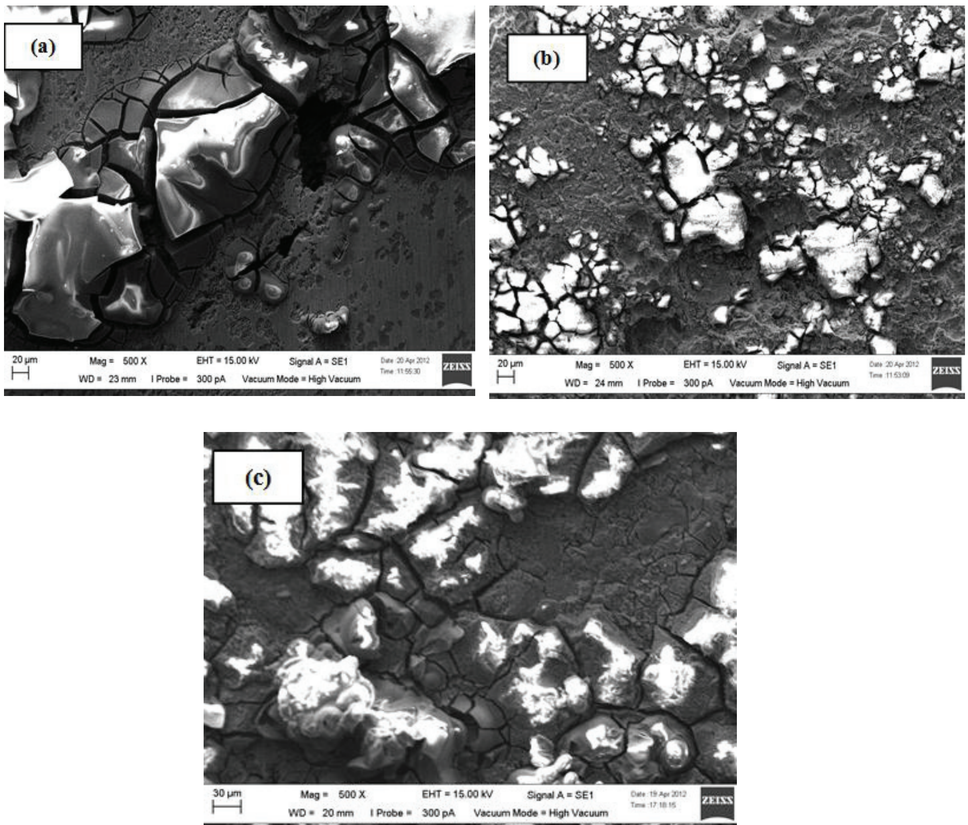

Figure 2: Corrosion attack morphologies for the (a) Al-Zn-Mg, (b) Al-Zn-Mg-Sn and (c) Al-Zn-Mg-Sn coated RuO_2 samples after 10 h of immersion in sea water.

3.2 Potentiodynamic Polarisation

Figure 3 shows the polarisation curves for the aluminium alloy samples. After the polarisation process, corrosion potential (E_{corr}) for (c) was found to be more electropositive than those of the (a) and (b) samples. This is due to the insufficient porosity ratio against the surface of substrate which impedes the charge movement, thus slowing down the electrochemical reaction at the alloy-solution interface. However, this obstacle can be further improved or optimised by heating the RuO_2 at approximately 400 °C as suggested by Shibli *et al.* (2007). Although (c) exhibited a more electropositive corrosion potential value than that of the (b) sample, there is no indication of any passivation behaviour occurring in the dissolution process as shown by the potentiodynamic plot. This phenomena is due to the porous and loose mud-like surface layer created by the RuO_2 coating, facilitating ionic movement and thus catalysing the active dissolution process (Shibli *et al.*, 2007; Jingling *et al.*, 2012).

The anodic curve for sample (a) showed a slight current plateau, which can be ascribed from the existence of a thick passive oxide layer on the alloy surface that can restrain the ionic-electron movement. However, due to the addition of 1.5%wt Sn, both samples (b) and (c) showed a smooth anodic current, with no passivation occurring. This observation clearly shows that Sn can play a very important role in weakening the oxide layer properties of both alloys by promoting more defect sites to be attacked by aggressive anions. This observation was also in good agreement with a previous study conducted by Umoru & Ige (2007). Sample (c) showed a better anodic activation curve which indicates the systematic breakdown of the protective oxide layer on the surface of the aluminium alloy substrate. Table 4 shows that higher corrosion current (I_{corr}) density was observed for sample (c) as compared to samples (a) and (b). The increase of corrosion rate for this sample is believed to be contributed by the presence of metallic RuO_2 coating on the Al-Zn-Mg-Sn alloy surface, which has synergistic effect in mobilising the ionic species and enhancing ion-electron movement, and thus, catalysing the electrochemical process.

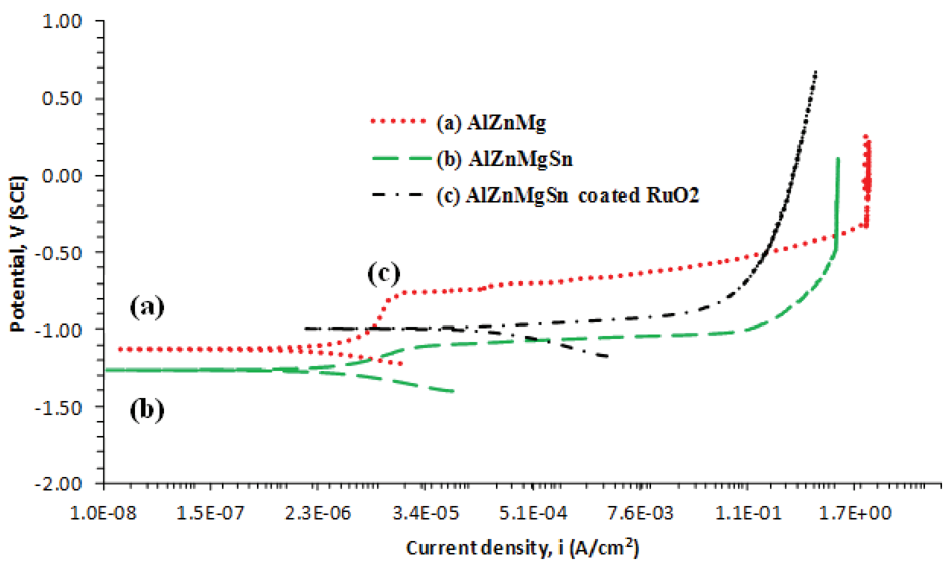

Figure 3: Potentiodynamic polarisation curves for the (a) Al-Zn-Mg), (b) Al-Zn-Mg-Sn and (c) Al-Zn-Mg-Sn coated RuO_2 samples in sea water.

Table 4: E_{corr} and I_{corr} values of the three aluminium alloys derived from the potentiodynamic curves in Figure 3.

Alloys	E_{corr} (V vs SCE)	I_{corr} ($\mu A/cm^2$)
Al-Zn-Mg	-1.130	3.00
Al-Zn-Mg-Sn	-1.270	5.09
Al-Zn-Mg-Sn coated RuO_2	-1.005	298.00

The higher corrosion current density for sample (c) indicates that active dissolution occurs in the system, which is usually dominated by uniform corrosion. The uniformity of corrosion attack morphology for Al-Zn-Mg-Sn has been reported by Mahdi *et al.* (2011), who found that Al-Zn-Mg-Sn alloys tend to form intermetallic particles known as Mg_2Sn. The presence of Mg_2Sn particles in the alloy will generate defects on the oxide layer by forming thin and weak oxide properties on the surface of the alloy. When exposed to aggressive chloride solution, this weak spot will became more vulnerable to chloride attack. This attack usually starts at the outer passive layer on top of the Mg_2Sn intermetallic particles (Jafarzadeh *et al.*, 2008).

3.3 Electrochemical Impedance Spectroscopy (EIS)

EIS is a very popular method which has been increasingly employed by a number of investigators to study electrochemical properties of aluminium alloy materials (Fidel *et al.*, 2006; Naseer & Khan, 2010; Mahdi *et al.*, 2012). The Nyquist plots for the early stages of immersion for samples (a), (b) and (c) in Figure 4 show a similar capacitive and resistive behaviour, reflecting the characteristics of passive oxide layer at the alloy-solution interface (Shibli *et al.*, 2007) with the plot for sample (c) exhibiting the lowest capacitive and resistive values. This means that the corrosion mechanisms of the samples are the same, except that their corrosion rates are different. For sample (c), an active interaction of ionic species occurred at the alloy solution interface, diffused through the alloy oxide layer (Mahdi *et al.*, 2010). The EIS diagram in Figure 4 also shows the presence of an inductive loop in the low frequency region (from 1 to 0.01Hz) for both samples (a) and (b) which can be ascribed from high current density accumulation and aggression of ionic species at the oxide-metal interface. The activation of sample (a) was due to the presence of fine intermetallics in the Al-Zn-Mg alloy, such as $Al_2Mg_3Zn_3$ compound, which later became active in the form of depolarisant sites that produce defective oxide film and enhance the alloy dissolution process (Bruzzone *et al.*, 1997; Orozco *et al.*, 2007).

For sample (b), the addition of Sn facilitated the alloy activation effect. Both samples (a) and (b) exhibited similar semicircle arc sizes, while sample (c) showed the smallest depressed capacitive loop features, which can be ascribed from the less resistive behaviour of the sample. Based on the EIS diagram, the presence of Sn in sample (b) was found to be not very effective in contributing to the activation process at the early stage of immersion. However, the presence of RuO_2 coating applied on the same alloy changed the impedance behaviour of the alloy by exhibiting low resistance to polarisation (R_p). This characteristic was believed to be due to the porous and cracked RuO_2 outer layer morphology which can facilitate and activate the electro-ionic movement process (Shibli & Gireesh, 2003; Shibli *et al.*, 2004, 2007). No inductive semicircle is observed for sample (c), which indicates that the sample dissolved uniformly, without pitting attack (Hoang & Phan, 2006).

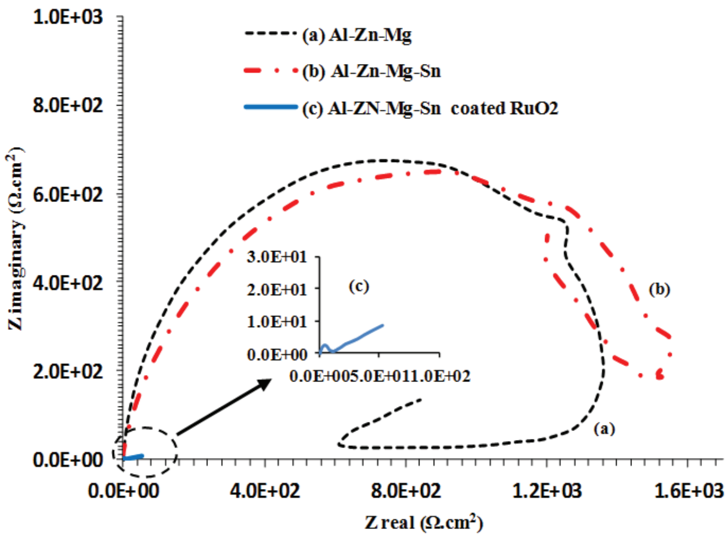

Figure 4: Nyquist plots obtained for the (a) Al-Zn-Mg, (b) Al-Zn-Mg-Sn and (c) Al-Zn-Mg-Sn coated RuO_2 samples at initial immersion in sea water. (Enlarged plot for sample (c) indicated by the arrow)

The Nyquist plot for sample (c) had a small distinctive capacitive loop at the high frequency region (from 10 to 100 kHz), which indicates the characteristics of the sample's surface homogeneity. The application of catalytic coating has been reported to suppress the formation of passive Al_2O_3 on aluminium alloy surfaces, which in turn provides a suitable surface morphology for the uniform dissolution process to take place (Shibli *et al.*, 2004, 2007, 2008).

At the low frequency region, the Nyquist plot showed a "Warburg like" behaviour, where the phase angle is constant at 45° and independent of frequency. The Warburg behaviour is the characteristic of diffusion or mass transport impedances of systems which traduce the ion penetration in the porous structure of the coatings. It also can be explained by the delay in progression of ionic movement through the RuO_2 layer, especially at the initial stage of immersion.

After 10 h of immersion in sea water, all three samples showed similar corrosion behaviour, but the corrosion process occurred at different rates. This can be clearly seen in Figure 5, where the smallest capacitive loop diameter was recorded by sample (c), followed by sample (b), with sample (a) having the biggest diameter. The Warburg tail behaviour was found to dominate in all three samples at the low frequency region (Liu *et al.*, 2005). Such a situation is considered normal due to the thickening of corrosion product with incremental period of the sample exposed to aggressive chloride media. This in turn will increase electrolyte diffusion through the coated layer as stated by Skale *et al.* (2008).

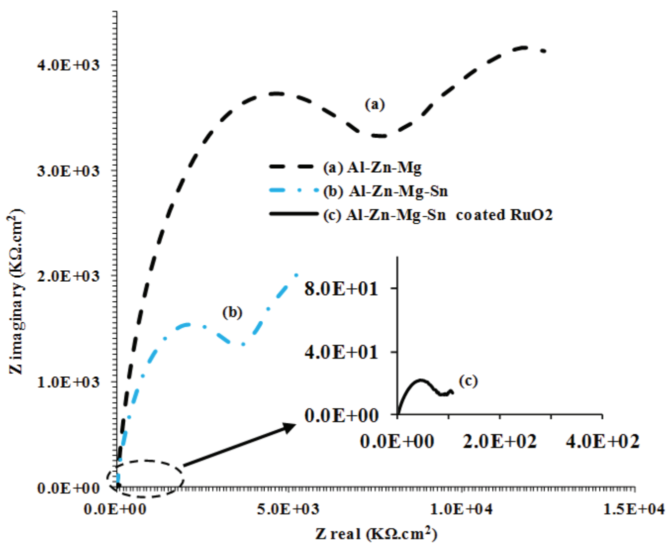

Figure 5: Nyquist plots obtained for the (a) Al-Zn-Mg, (b) Al-Zn-Mg-Sn and (c) Al-Zn-Mg-Sn coated RuO_2 samples at 10 h immersion in sea water. (Enlarged plot for sample (c) indicated by the arrow)

The resistive behaviour of the samples' surfaces at initial and 10 h of immersion can be seen clearly from Bode plots shown in Figures 6 and 7 respectively. At the low frequency region, sample (c) was found to exhibit the lowest R_p values as compared to samples (a) and (b), as this sample is very reactive and dissolves easily in the chloride solution. This finding is in agreement with the potentiodynamic polarisation test and the corrosion morphology in Figure 2(c), which showed a loose and crack mud-like outer layer that can provide better ionic species movement and interaction for the corrosion process.

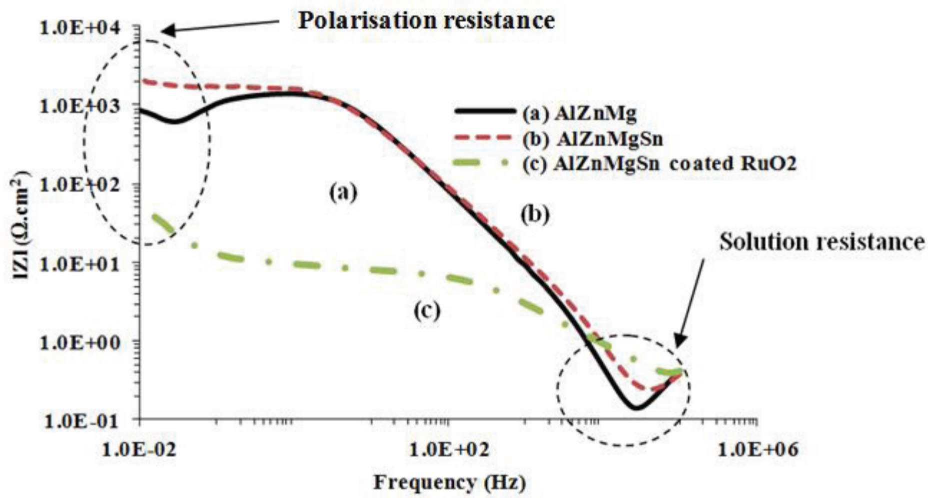

Figure 6: Bode plots obtained for the (a) Al-Zn-Mg, (b) Al-Zn-Mg-Sn and (c) Al-Zn-Mg-Sn coated RuO_2 samples at initial immersion in sea water.

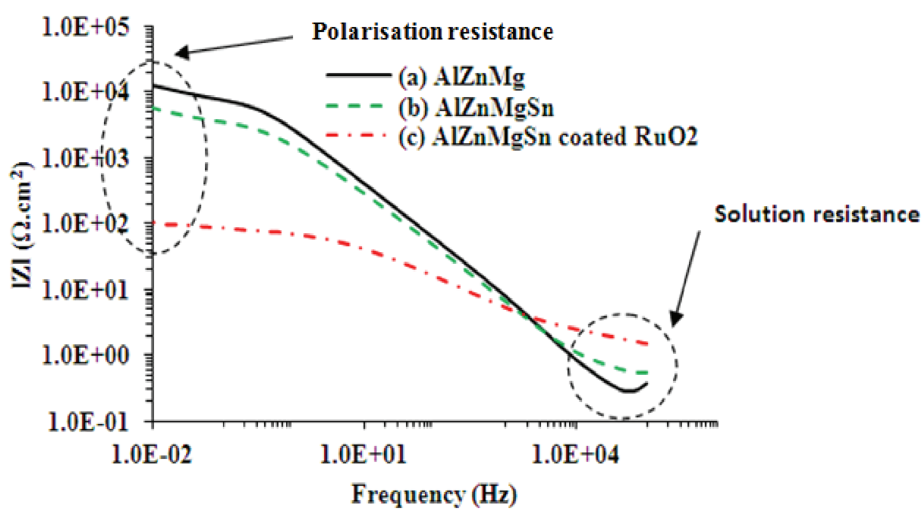

Figure 7: Bode plots obtained for the (a) Al-Zn-Mg, (b) Al-Zn-Mg-Sn and (c) Al-Zn-Mg-Sn coated RuO_2 samples at 10 h of immersion in sea water.

Equivalent electrical circuit models (Junguang *et al.*, 2011; Jingling et al. 2012) were proposed to simulate the electrical behaviour at the alloy-solution interface at initial and 10 h of immersion. A series of models, as shown in Figures 8-10, were employed and circuit elements, such as capacitance (C), inductance (L) and resistance (R), were introduced to ascribe the double-layer capacitance behaviour of the system. In order to obtain a more precise fitting, this capacitance element was replaced by a constant phase element (CPE). The impedance of a CPE is defined by following equation (Jingling & Jiuba, 2010):

$$Z(j\omega) = (Y_o)^{-1} (j\omega)^{-n} \tag{1}$$

where Y_o is the CPE constant, j is the imaginary unit, n is the CPE power ($0 < n < 1$), and ω is the angular frequency ($\omega = 2\pi f$, f is the frequency). The CPE is pure capacitance when n is 1. For a capacitance element, the deviation of n from the units is due to heterogeneous effects. In Figures 8-10, R_{sol} is the solution resistance used as the electrolyte between the working and reference electrodes, CPE_{po} is the CPE through pores on the RuO_2 catalytic coating, R_p is polarisation resistance, CPE_{dl} is the CPE at substrate / passive layer interphase, R_{po} is the pore resistance on the catalytic coating, CPE_{pit} is the CPE at pitting dissolution area, L_{pit} is an inductance combined with R_{pit} ascribing pitting resistance due to corrosion product accumulation at the pitted area opening, and Warburg W_{pit} ascribes the diffusion of electrolytes through the catalytic coating.

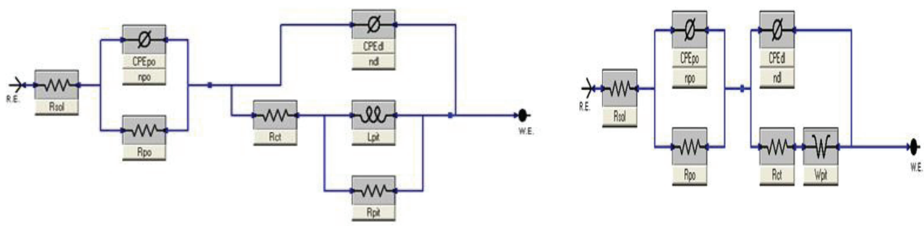

(a) **(b)**

Figure 8: Proposed equivalent circuit model for the Al-Zn-Mg sample in sea water for (a) initial and (b) 10 h of immersion.

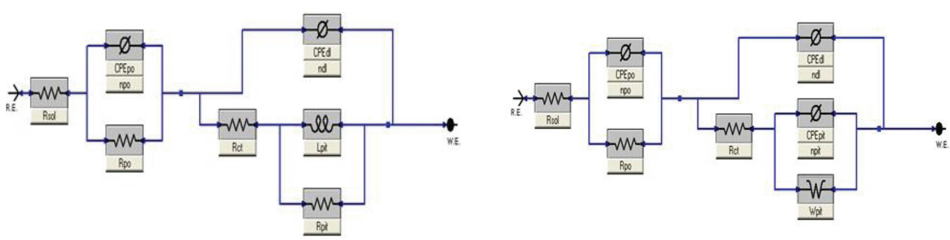

(a) **(b)**

Figure 9: Proposed equivalent circuit model for the Al-Zn-Mg-Sn sample in sea water for (a) initial and (b) 10 h of immersion.

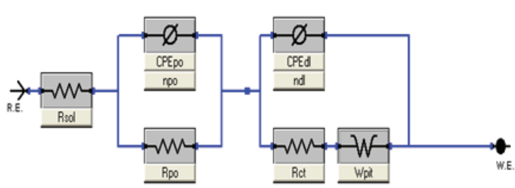

Figure 10: Proposed equivalent circuit model for the Al-Zn-Mg-Sn sample coated with RuO_2 in sea water for both initial and 10 h of immersion.

Figures 11-13 shows the experimental and fitted Bode plots for the samples exposed to sea water at initial and 10 h of immersion by using the proposed equivalent circuit models. It can be seen that there is a good correspondence between the experimental and simulated data, and it is possible to interpret that all circuit elements on the models produce significant information related to the electrical properties of the system.

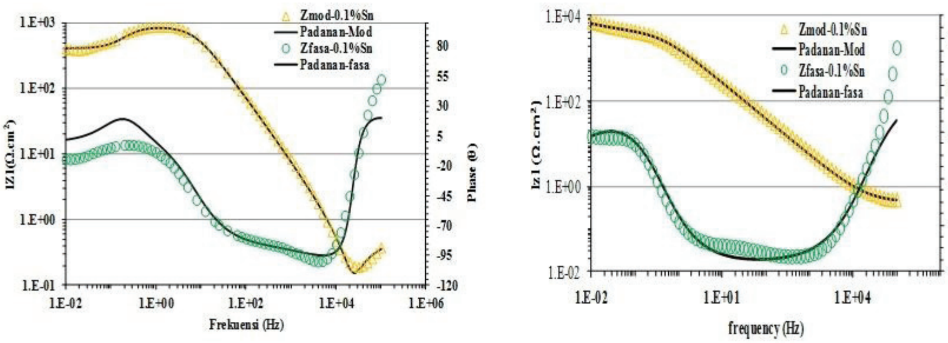

(a) **(b)**

Figure 11: Simulated and experimental data in Bode plots for the Al-Zn-Mg sample in sea water for (a) initial and (b) 10 h of immersion.

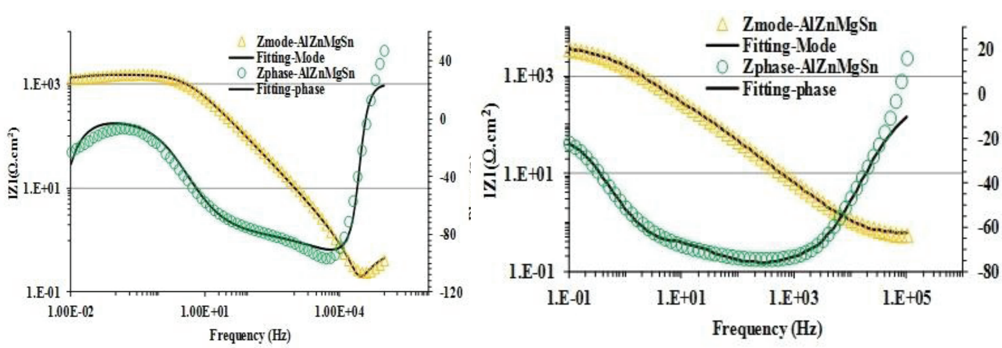

(a) **(b)**

Figure 12: Simulated and experimental data in Bode plots for the Al-Zn-Mg-Sn sample in sea water for (a) initial and (b) 10 h of immersion.

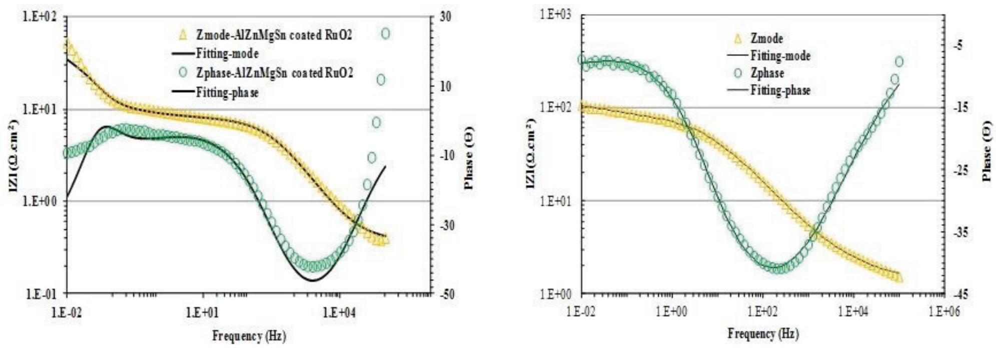

(a) **(b)**

Figure 13: Simulated and experimental data in Bode plots for the Al-Zn-Mg-Sn coated RuO_2 sample in sea water for (a) initial and (b) 10 h of immersion.

The optimised EIS modelling values for every circuit element in the circuit were obtained by using the non-linear least square (NLLS) fitting method as shown in Table 5. The highest value of R_p was recorded for sample A. The R_p value is directly associated with the electrochemical corrosion rate value (Jingling & Jiuba, 2010), whereby higher R_p values indicate lower rate material dissolution occurring in the system, which usually contributes to passivation behaviour. At initial immersion, an inductive loop at the low frequency region appears for samples A and B. The inductive loop may represent the pitting attack on corroded surface morphology (He *et al.*, 2011). The usage of R_{pit} and L_{pit} in the circuit is ascribed from the presence of the pitting process in the system (Jingling & Jiuba, 2010; Jingling *et al.*, 2012).

Table 5: Simulated EIS values for aluminium alloy in natural sea water for initial and 10 h of immersion.

Parameters	Initial Immersion			10 h of immersion		
	A	B	C	A	B	C
R_{sol} (Ω.cm²)	1.5	2.55	0.37	0.41	0.96	1.1
R_{po} (Ω.cm²)	0.66	0.14	7.77	82.7	45.5	70.8
CPE_{po} (µS.cm²)	1.15	6.84	0.04	0.16	2.88	0.001
n_{po}	0.52	0.006	0.74	0.32	0.0001	0.61
R_p (Ω.cm²)	940	692	6.40	990	340	156
CPE_{dl} (µS.cm²)	0.29	0.4	0.00003	0.58	0.01	0.05
n_p	0.94	0.87	0.55	0.89	0.82	0.30
L_{pit}	540	11200	-	-	-	-
R_{pit} (Ω.cm²)	615	857	-	-	-	-
W	-	-	0.16	0.09	0.21	2.82
CPE_2	-	-	-	-	0.22	-
n_2	-	-	-			

A: Al-Zn-Mg
B: Al-Zn-Mg-Sn
C: Al-Zn-Mg-Sn coatedRuO_2

The preferred dissolution morphology was general attack rather than pitting, since pitting attack has been correlated to less than optimal performance (Ganesca & Juarez, 2000). From this study, it is clear that aggressive dissolution and uniform attack can be achieved by using Ru as the coating material based on its low R_p value as compared to the other samples (Table 5). The SEM image in Figure 2(c) further highlights the absence of pitting mechanism in the dissolution process by showing only a cracked surface rather than severe pitting morphology. This cracked surface further facilitates the charge movement, explaining the high corrosion current density as shown in Table 4.

4. CONCLUSION

In this study, both Sn and RuO_2 have proved their role in activating aluminium alloys in natural sea water. The presence of alloying element Sn (1.42%wt.) in the Al-Zn-Mg alloy produced voltage difference at the alloy surface due to the cathodic nature of Sn as compared to Al matrix and thus initiated corrosion attack by localised dissolution. The presence of Sn also reduced the stabilisation period of OCP from 45 ks to only 2 ks. As for the RuO_2 coated Al-Zn-Mg-Sn alloy, it successfully overcame the tendency of localised attack or pitting corrosion on the alloy surface by acting as a good catalytic activator layer for producing uniform and continuous dissolution process with no sign of passive behaviour as indicated from the potentiodynamic measurement. The impedance study showed that the presence of RuO_2 on the alloy surface can be very useful in reducing polarisation resistance R_p of Al-Zn-Mg-Sn alloy at the early stage of immersion and maintaining ionic movement even after 10 h of immersion. The RuO_2 coating has shown its usefulness by modifying the electrical properties of Al-Zn-Mg-Sn oxide layer by forming a porous and loose outer layer at the surface of the alloy. Higher dissolution rates as shown by low R_p values in this study are indicative that this type of alloy (Al-Zn-Mg-Sn coated with RuO_2) poses excellent electrochemical behaviour for sacrificial anode material in cathodic protection systems.

ACKNOWLEDGEMENT

The authors would like to thank the Science and Technology Research Institute for Defence (STRIDE) for providing research facilities and technical assistance. We also acknowledge the academic and technical staff from the School of Materials Engineering, University Malaysia Perlis (UniMap), for technical assistance and a series of fruitful discussions. The authors also gratefully acknowledge officers and staff from the Ship Technology Branch, Maritime Technology Division, STRIDE, for their help and cooperation in completing this paper.

REFERENCES

Andrea, M., Marie-Laure, M., Samuel, P., Daniel, B. & Christille, C. (2011). Assessment of sacrificial anode impact by aluminum accumulation in mussel Mytilus edulis: A large-scale laboratory test. *Mar. Pollut. Bull.,* **62**: 2707–2713.

Barbucci, A., Cerisola, G., Bruzzone, G. & Saccone, A. (1997). Activation of aluminium anodes by the presence of intermetallic compounds. *Electrochim. Acta,* **42**: 2369-2380.

Bessone, J. B. (2006). The activation of aluminium by mercury ions in non-aggressive media. *Corros. Sci.,* **48**: 4243 – 4256.

Bruzzone, G., Barbucci, A. & Gerisola, G.(1997). Effect of intermetallic compounds on the activation of aluminium anodes. *J. Alloy Compd.*, **247**: 210-216.

Feng,Y., Wang,, R., Yu, K., Peng, C.& Li, W. (2007). Influence of Ga and Hg on microstructure andelectrochemical corrosion behavior of Mg alloy anode materials. *T. Nonferr. Metal Soc.,* **17**: 1363-1366.

Feng, Y., Wang, R., Yu, K., Peng, C. & Li, W (2008). Influence of Ga Content on Electrochemical Behaviorof Mg-5 at%Hg Anode Materials. *Mater T JIM: Special Issue on Platform Science and Technology for Advanced Magnesium Alloys, IV,* **49**: 1077 - 1080.

Fidel, G., Juan, M., Ruben, D. & Genesca, J. (2006). Electrochemical study on magnesium anodes in NaCl and $CaSO_4$–$Mg(OH)_2$ aqueous solutions. *Electrochim Acta*, **51**: 1820–1830.

He, J., Wen, J.,Li, X., Wang, G. & Xu, C.(2011). Influence of Ga and Bi on electrochemical performance of Al-Zn-Sn sacrificial anodes. *T Nonferr Metal Soc*, **21**: 1580-1586.

Hoang, T.B.T. & Phan, L.C. (2006). Performance of the zinc sacrificial anode in concrete environment. *14th Asian-Pacific Corrosion Control Conference*,October 21-24, 2006, Shanghai, China.

Idusuyi, N. & Oluwole, O.O. (2012). Aluminium anode activation research - A review. *Int. J. Sci. Tech.*, **2**(8): 561-566

Umoru, L.E. & Ige, O.O. (2007). Effects of Tin on Aluminum – Zinc – Magnesium Alloy as Sacrificial Anode in Seawater. *J. Min. Mat. Charact. Eng.,* **7**: 105-113.

Jingling, M. & Jiuba, W. (2010). Corrosion analysis of Al–Zn–In–Mg–Ti–Mn sacrificial anode alloy. *J. Alloy Compd.*, **496**: 110–115.

Jingling, M., Jiuba, W., Wenxia, Z. & Quanan, L. (2012). In situ corrosion analysis of Al-Zn-In-Mg-Ti-Ce sacrificial anode alloy. *Mater. Charact.*,**65**: 86–92.

Jiuba, W., Junguang, H. & Xianwen, L. (2011). Influence of silicon on the corrosion behaviour of Al–Zn–In–Mg–Ti sacrificial anode. *Corros. Sci.*, **53**: 3861–3865.

Genesca, J. & Juarez, J. (2000). Development and testing of galvanic anodes for cathodic protection. *Contrib. Sci.*, **1**: 331-343.

Junguang H., Jiuba, W. & Xudong, L. (2011). Effects of precipitates on the electrochemical performance of Al sacrificial anode. *Corros. Sci.*, **53**(5): 1948-1953.

Jafarzadeh, K., Shahrabi, T. & Hosseini, M.G. (2008). EIS Study on Pitting Corrosion of AA5083-H321 Aluminum-Magnesium Alloy in Stagnant 3.5% NaCl Solution. *J. Mater. Sci. Technol.*, **24**(2): 215-219.

Likun, X., Yonglei, X. & Juntao, W. (2009). A comparative study on IrO_2–Ta_2O_5 coated titanium electrodes prepared with different methods. *Electrochim. Acta*, **54**: 1820-1825.

Liu, J., Gong, G. & Yan, C. (2005). EIS study of corrosion behaviour of organic coating/Dacromet composite systems. *Electrochim. Acta*, **50**: 3320–3332.

Jingling, M.A., Wen, J., Gengxin, L.I. & Chunhua, X.V. (2010). The corrosion behaviour of Al–Zn–In–Mg–Ti alloy in NaCl solution. *Corros. Sci.*, **52**: 534–539.

Naseer, A. & Khan, A.Y. (2010). Electrochemical impedance spectroscopicstudies of thepassive layer on the surface of copper as a function of potential. *Turk. J. Chem.*, **34**: 815 – 824.

Mahdi, C.I. Daud, A.R., Mohd Yazid, A., Daud, M., Shamsudin, S.R., Nik Hassanuddin, N.Y., Mohd Subhi, D.Y. & Mohd Moesli, M. 2012). An Electrochemical Impedance Spectroscopy Study of Al-Zn and Al-Zn-Sn Alloys in Tropical Seawater. *Key Eng. Mat.,* **510-511**: 284- 292.

Mahdi, C.I., Mohd Subhi, D.Y., Nik Hassanuddin, N.Y., Mohd Fauzi, M.N., Mohd Moesli, M., Osmera, I. & Irwan, M. (2011). Electrical characterization og As-Cast Al-Zn-Sn alloys for corrosion control application in tropical marine environment. *Defence S&T Tech. Bull.*, **4**:119-130.

Mahdi,C.I., Ahmad, M.Y. , Daud, A.R. & Daud, M. (2010). The Effect of Sn on the Impedance Behaviour of Al-Zn Alloys in Natural Chloride solution. *Key Eng. Mat.*, **442**: 322-329.

Qingfeng, L. & Niels, J.B. (2002). Aluminum as anode for energy storage and conversion: a review. *J. Power Sources*, **110**:1–10.

Orozco, R. , Ganesca, J. & Juarez-Islas, J. (2007). Effect of Mg Content on the Performance of Al-Zn-Mg Sacrificial Anodes. *J. Mater. Eng. Perform.*, **16**: 229-235.

Shibli, S.M.A., Gireesh, V.S. & Sony, G. (2004). Surface catalysis based on ruthenium dioxide for effective activation of aluminium sacrificial anodes. *Corros. Sci*, **46**(4):819-830.

Skale, S., Dolecek, S. & Slemnik, M. (2008). Electrochemical impedance studies of corrosion protected surfaces covered by epoxy polyamide coating systems. *Prog. Or. Coat.,* **62**: 387–392.

Shibli, S.M.A. & Gireesh, S. (2007). Electrochemical impedance spectroscopic analysis of activation of Al–Zn alloy sacrificial anode by RuO_2 catalytic coating. *Appl. Surf. Sci.,* **253**: 7510–7515.

Shibli, S.M.A. & Gireesh, V.S. (2005). Activation of aluminium alloy sacrificial anodes by selenium. *Corros. Sci.*, **47**: 2091–2097.

Shibli, S.M.A., Gireesh, V.S. & Sony, G. (2004). Surface catalysis based on ruthenium dioxide for effective activation of aluminium sacrificial anodes. *Corros. Sci.*, **46**: 819–830.

Shibli, S.M.A., Archana, S.R. & Muhamed Ashraf, P. (2008). Development of nano cerium oxide incorporated aluminium alloy sacrificial anode for marine applications. *Corros. Sci.*, **50**: 2232–2238.

Shibli, S.M.A. & Gireesh, V.S. (2003). Surface activation of aluminium alloy sacrificial anodes by IrO_2. *Appl. Surf. Sci.*, **219**: 203–210.

Shibli, S. M. A., Dilimon, V. S. & Saji, V. S. (2007). RuO_2–TiO_2 mixed oxide composite coating for improvement of Al-alloy sacrificial anodes. *J. Solid State Electr.*, **11**: 201–208.

Defence S&T Tech. Bull., 6(2): 93-110, 2013

MANAGEMENT OF NAVAL VESSELS' ELECTROMAGNETIC SIGNATURES: A REVIEW OF SOURCES AND COUNTERMEASURES

Hasril Nain*, Mahdi Che Isa, Mohd Moesli Muhammad, Nik Hassanuddin Nik Yusoff, Mohd Subhi Din Yati & Irwan Mohd Nor

Materials Research Group, Maritime Technology Division (BTM), Science & Technology Research Institute for Defence (STRIDE), Ministry of Defence, Malaysia

*Email: hasril.nain@stride.gov.my

ABSTRACT

This paper provides a broad overview of underwater electromagnetic signaturesthat are produced by naval vessels. There are four components of electromagnetic signatures on vessels, static (SE) and alternating electric (AE), and static (SM) and alternating magnetic (SM), that can be detected by sea mines.Effective measures for electromagnetic signature management are required to protect vessels from being detectedby sea mines.Techniquesthat are normally used in controlling, reducing and eliminating unwanted electromagnetic signature, including degaussing (DG), deperming, shaft grounding, cathodic protection,material choices for vessel construction and positioning of equipment in vessels,are also discussed.

Keywords: *Sea mines; electromagnetic signatures; direct (DC) and alternating (AC) current components; stray fields; electromagnetic countermeasures.*

1. INTRODUCTION

One of the most effective weapons against naval vessels in littoral waters is sea mines. In the last 20 years, sea mines have damaged 17 US Navy vessels, whereas air and missile attacks have damaged only four. During the Korean War, mines laid by North Korean forces damaged 11 US naval vessels. Since World War II, sea mines have caused more damage to US warships than all other weapons systems combined (DOD, 2007). Surface vessel and submarine electromagnetic signatures have been exploited for over 80 years by mines, using both underwater and airborne surveillance systems (Holmes, 2006). This shows that seamines are an immanent threat to naval vessels. In addition to being effective, sea mines are relatively inexpensive and represent an asymmetric threat.

Seamines can be found throughout the water column and / or within seafloors, and comes in different types. Moored mines, which have been available in militaries since World War I, remains a potent weapon, having damaged the Samuel B. Roberts and USS Tripoli warships in 1988 and 1991 respectively (Morison, 1995). A moored mine floats beneath the surface of the ocean, tethered to the bottom by an anchor. It typically detonates upon direct physical contact with a vessel or through a relative influence signature mechanism. However, this type of mine has a weakness; for example, China's EM 31and EM 32 models, are limited by the length of their mooring cables or chains to waters shallower than 200 m (Watts, 2005). This makes them easy to sweep, even by unsophisticated minesweepers, once their presence is known. Drifting mines, also known as free floating mines, are primarily used to attack medium and small surface vessels when sailing, or anchored at bridges or ports. It can be laid by military or civilian vessels. Drifting mines are not restricted by water depth or sea area, and may frequently float out of the maritime battle space, and can destroy nonbelligerent countries' vessels. Therefore, international treaties ban the use of drifting seamines (Changsheng, 2005). Bottom mines are mines laid directly on the seabed and detonate when they sense influence signatures from vessels that satisfy their triggering criteria (Glosny, 2004). These mines are dangerous and very effective weapons,which can have vessel counting features. For example, China's Type 500 and 1,000 bottom mines can let up to 15 vessel signatures pass before denoting. They also have activation delay mechanisms that allow their placement for up to 250 days before arming, and self destruction timers that can be set for up to 500 days (Hewson, 2005). This type of mine is difficult to detect and remove from waters as compared to moored mines (Hartmann & Truver, 1991). However, as these mines have limited sensing ranges and charges, they are only confined to oceans of 250 m and below (Watts, 2005).

Sea mines are often triggered by the electromagnetic field of a passing naval vessel. Simple sea mines use induction coils to sense the static magnetic field of an oncoming vessel. They have limited processing capability and hence, their ability to target specific vessels classes or avoid minesweeping measures is also very limited. Modern mines have greatly improved on the capabilities of these early mines with the introduction of thin film and fluxgate magnetometers. Modern magnetic sensors are more reliable and have a greater range (Castles, 1997). It is equipped with multichannel exploders fitted with sensors responding to such physical fields of vessels, including magnetic (induction), acoustic, hydrodynamic (pressure) and electric (Proshkin, 2011). Figure 1 shows a MR80/B sea mine which is used by the Royal Malaysian Navy (RMN) and its electronic module that consists of sensors to detect signatures of vessels. This mine is also equipped with facilities to detect and destroy underwater minesweepers that are normally operated ahead of vessels.

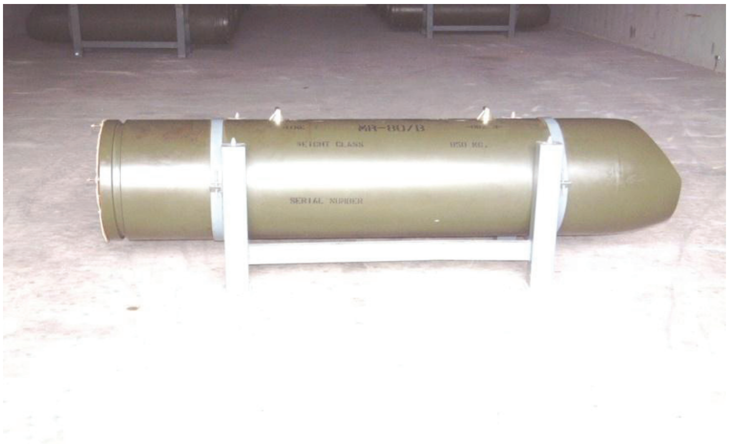

(a)

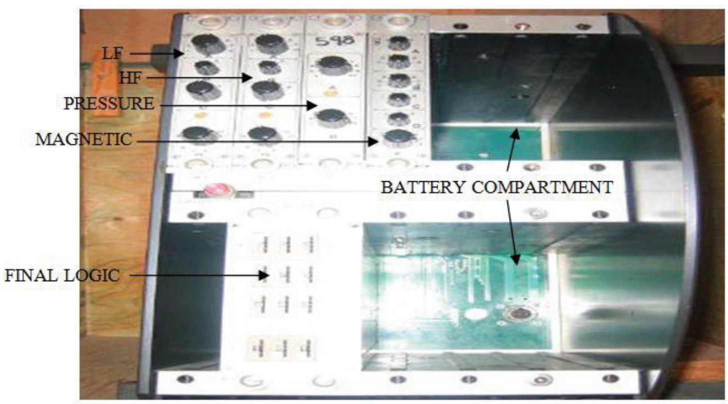

(b)

Figure 1: (a) A MR80/B sea mine and (b) its electronic module. LF and HF stand for low and high frequencies respectively.
(Source: RMN, 2011)

As all vessels emit electromagnetic fields, which are propagated through water, they are susceptible to being detected by underwater sensors or mines (Rodrigo & Sanchez, 1990). Therefore, electromagnetic signatures of vessels need to be kept below the safe level, which is the maximum level of electromagnetic signatures that a vessel can have in order for it to sail safely over sea mines. The safe level is dependent on sea mines' sensitivity and distance of the vessel from seamines (RMN, 2005). Navies have been practicing various countermeasures to avoid their vessels from detected by sea mines, which take the form of devices to substantially eliminate static and alternating components of electromagnetic signatures, thereby removing the mine's ability to classify the vessel's electromagnetic signatures (Jeffrey & Brooking, 1999).

This paper will discuss the importances of the electromagnetic signature management for vessels. It will provide a broad overview of underwater electromagnetic signatures that are produced by naval vessels. The techniques normally used for controlling, reducing and eliminating unwanted electromagnetic signature by navies in order to protect vessels from sea mines are also discussed.

2. ELECTROMAGNETIC SIGNATURES FIELD

Underwater electromagnetic signature fields can be separated into four components (Figure 2): two direct current (DC) terms, static electric (SE) and magnetic (SM); and two alternating current (AC) terms, alternating electric (AE) and magnetic (AM).

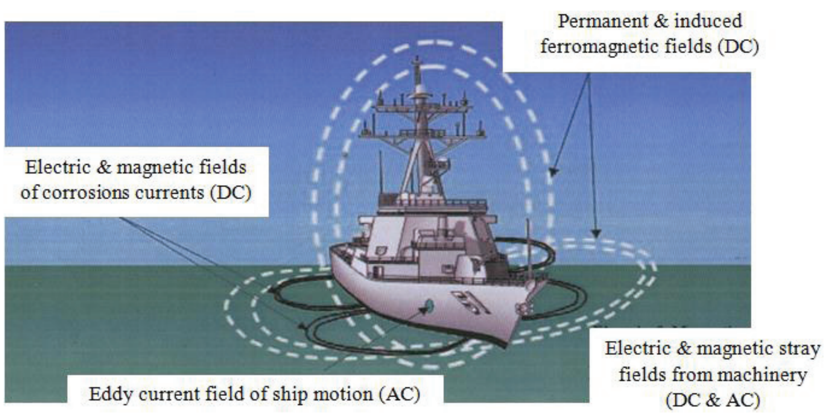

Figure 2: Underwater electromagnetic signatures of a naval vessel. (Adapted from McElman (2007))

2.1 DC Components

SE is referred to as underwater electric potential (UEP) and is characterised by its amplitude, which as observed from a static sensor, is almost constant (while the SE field magnitude remains constant, the effect of variable distance for the vessel in movement implies that the magnitude of the field measured by the sensor varies slightly with time). The range of considered frequencies is typically lower than 2 Hz (Rodrigo & Sanchez, 1990). The SE signature is associated with electric currents in connection with the electric field caused by corrosion currents coupled with the magnetic field, which is called the corrosion related magnetic (CRM) signature (Birsan, 2010). SE signatures arise from the creation of electric dipoles along the hulls of vessels (bare steel, anodes and propellers) (Figure 3), as well as currents in seawater from the movement of ions from anodic sources of dissimilar metals (steel in hull and hull appendages) and impressed current cathodic protection (ICCP) anodes to cathodic sources of dissimilar metals (sodium bromide and other metals in propellers) (Diaz *et al.,* 2001).

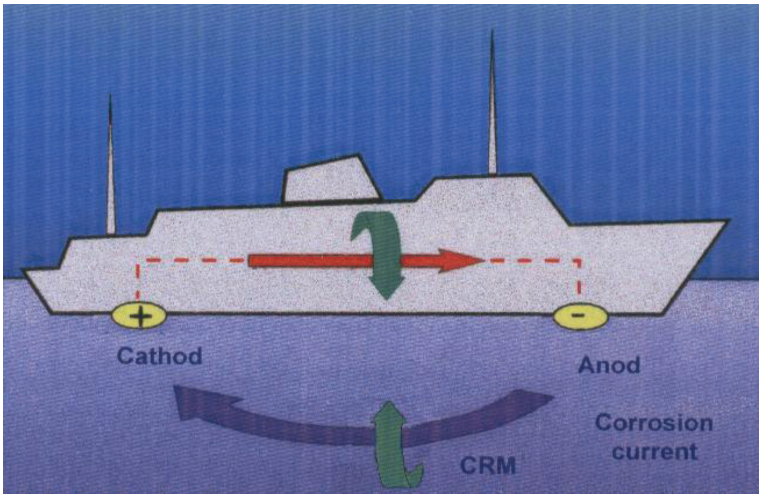

Figure 3: SE signatures on the hull of a vessel.
(Source: Birsan (2010))

The SM field arises from the disturbance of the earth's magnetic field when a vessel with significant ferrous content is placed in it. There are two major components of this SM field source (Holmes, 2006):

1. Induced magnetism from the ferrous content of the ship (permeability), the earth's magnetic field, and the shape and orientation of the vessel in the magnetic's field. If the magnetic permeability is very high, the material is ferromagnetic. These factors cause the ferrous material on vessel to act as a magnet in the presence of the earth's magnetic field. The higher permeability and / or stronger the earth's magnetic field, the stronger the magnet. The shape and orientation of the vessel also tend to enhance induced magnetism. Longer vessels which are parallel to the earth's magnetic field can also create stronger magnetism.

2. Permanent magnetism of the vessel which was created inadvertently during construction of the ship, changed inadvertently during rough travelling and combat operations, and / or changed purposefully during the vessel's magnetic treatments.

Another source of the SM field is hull structure magnetic signature due to currents returning through the hull structure. This SM signature arises from the return flow currents in the shaft and hull structure from the propeller to the anodic sources (steel in hull and hull appendages, sacrificial anodes, and / or ICCP power supplies) (Figure 4). The SM field is also caused by CRM signatures from the creation of currents in seawater from the of ions from anodic sources and ICCP anodes to cathodic sources.

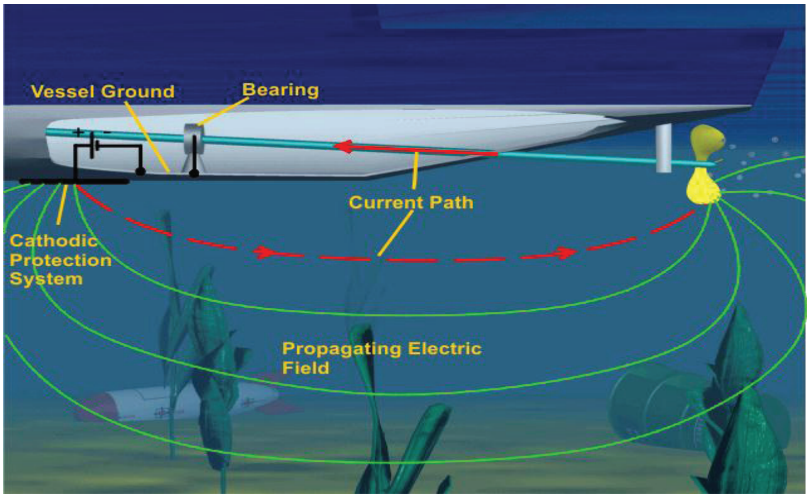

Figure 4: SM signature created by return current flow.
(Source: Mason (2009))

2.2 AC Components

The AE field, known as extremely low frequency electric (ELFE) field, arises due to the changing resistance between the shaft and hull as the propeller rotates. This resistance causes modulation of the current in the shaft and hull, with all of these components modulating at the same harmonic frequencies (Torrance, 2005). This source also contributes to AM signatures (Holmes, 2006).

The current ripple of the output of the ICCP's power supply is also one of the contributors of the AE and AM fields. These signatures arise from the modulating effect of the output current being injected into seawater from the ICCP anodes. The current modulation causes modulating AE and AM signatures at the same frequencies as the current ripple and harmonics (Diaz &Tims, 1999).

AM signatures occur when a vessel with significant continuous conductive surface areas is moving in the Earth's magnetic field in a such a way as to change the conductive area perpendicular to the direction of the magnetic field. This creates eddy currents in the conductive surfaces, which in turn, creates magnetic fields much like current through coils. These currents are alternating, creating AM fields (Figure 5).

Figure 5: Eddy current flow induced in a vessel's conducting hull due to its roll in the earth's magnetic field.
(Source: Holmes (2008))

There are two major contributors to the AM field source (Holmes, 2006):

1. The rolling and pitching of the vessel. The pitching of the vessel causes the magnetic field in the vertical and longitudinal directions to change, where the vertical field increases and the longitudinal field decreases during bow upward pitching movement on a north heading. The rolling of the ship causes the magnetic fields in the vertical and athwartship directions to change as a function of the angle of the roll.

2. Orientation and location of the vessel in the earth's magnetic field (latitude and heading). The vertical magnetisation remains constant within the same degree of latitude during course tracking, provided that there is a calm sea. The athwartship magnetisation changes with the vessel's course with maximum values for east and west headings, and zero crossings for north and south headings. On the other hand, longitudinal magnetisation has maximum values for north and south headings, and zero crossings for east and west headings.

2.3 Stray Fields

The last of electromagnetic sources on vessels is called the stray field. This field exists in entire fields of SE, AE, SM and AM. Stray field signatures are produced by any current carrying electric circuit found on board a vessel. Larger stray fields are produced by the electro-mechanical machinery and power distribution system of the vessel. High power electric generators, motors, switchgear and breakers, and distribution cables are also main contributors of the field (Holmes, 2006). These equipment produce currents during operation and increase the vessel's electromagnetic signatures.

3. ELECTROMAGNETIC SIGNATURE COUNTERMEASURES

One way to reduce the electromagnetic signatures of a vessel is to eliminate the respective sources or to provide a suitable system to protect them from unwanted electromagnetic influences (Holmes, 2006). A number of techniques exist that are designed to eliminate or reduce electromagnetic signatures of vessels in order to avoid detection or triggering a sea mine. This section will discuss the key methods to evade magnetic detection.

3.1 Degaussing (DG)

DG is the name given to the process of counteracting a vessel's magnetic field by using electromagnetic coils to generate a field equal but opposite to the natural magnetic signature (Davidson *et al.*, 1998). The application of DG systems started during World War II to protect naval vessels from magnetic mines and torpedoes (BHE, 2009). Recovery of one of the mines confirmed that the firing mechanism was triggered by a vessel's magnetic field and hence, the race to develop signature reduction technologies, such as DG systems, ensued within the British Admiralty and later, the US Navy. By the end of the war, more than 12,600 military and merchant vessels in the US fleet were equipped with DG systems (Poteete, 2010).

Shipboard DG systems are composed of loops of electric cables that, when energised with proper current, can cancel or reduce a vessel's magnetic signature. Initially, these systems were designed only to compensate induced and permanent magnetisation. A DG system must be able to compensate the three orthogonal components of vessel magnetisation, longitudinal (L), athwartship (A) and vertical (V) (Figure 6), independently from each other. There are two types of DG coils, VAL (vertical, athwartship, longitudinal) and MFQ (main, forecastle, quarter-deck). VAL DG coils are suitable for vessels that berth or sail in equatorial regions, while MFQ DG coils are suitable for the northern and southern regions. Advanced DG methods take this process one step further by increasing the number of on-board DG coils, and using sensors to measure the magnetic field of the vessel and actively eliminating it. In order to measure the magnetic field of a vessel at a DG range facility, the vessel is moved over the sensor arrays at constant speed at fixed headings. As the ship passes, the sensors are scanned at regular intervals and measurement data of magnetic signatures are obtained. Computer technology can therefore correct for the changes that occur over time to the magnetism of the vessel by adjusting the number of coils in on-board DG coils (MOD, 2008)

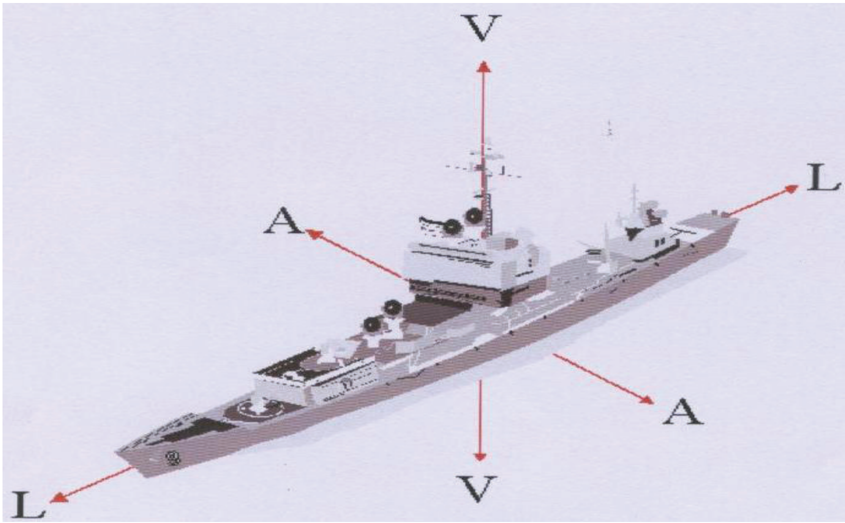

Figure 6: Coordinate system of a vessel's magnetisation. (Source: Birsan (2008))

The Lumut RMN base has a DG range facility to counter the magnetic influence of warships (Figure 7). The DG range is designed with two overrun ranges, measuring at 9 and and 18 m. The 9 m range is used for small vessels, while the 18 m range is used for large vessels. The system can be divided into three main components; offshore, onshore, and communications and navigation system. The offshore components consist of six tri-axis underwater sensors, three magnetic sensors for the 9 m range with 9 m depth from the sea surface, and two magnetic sensors for the 18 m range with 18 m depth. A pressure sensor is placed at 5 m depth to measure the depth of ranging during measurements. The onshore equipment consists of an electronic cabinet and computer, including the DG software, while the communications and navigation system contains a differential Global Positioning System (DGPS) system with laptop and very high frequency (VHF) radio (RMN, 2003. 2005).

Before the degaussing process is started, the DGPS system has to be installed on the vessel to monitor the vessel's movement over the sensors. The DG system onboard must be inspected by an authorised technician before performing magnetic measurement and treatment on the DG range. The magnetic signature of the vessel is captured by the sensors as the vessel passes over the sensor array. The vessel will pass over the sensor array from north to south and south to north headings in order to get the primary electromagnetic signature before the treatment process is implemented. Normally, the DG process takes a number of hours or days; for example, a newly built or refitted vessel will take about five days to complete. However, the availability of the DG system onboard is a main factor to achieve a minimum or required signature. Some vessels still using analog type DG systems instead of computerised systems. In this case, the DG technician needs to adjust the coils at each junction box located at different places onboard the vessel as required during magnetic ranging. The DG officer will inform the technician on the locations and number of coils that need to be adjusted according to the DG software's recommendation at the onshore laboratory. In comparion, for computerised DG systems, the technician only changes the number and current value of DG coils on the DG system controller that is located onboard the vessel. The underwater sensors need to be cleaned frequently due to marine borers, which can damage the sensors and affect the measurement results. The navigation system for the DG range is also of high concern, as the measurement cannot be implemented if the DGPS signal is too weak, such as due to poor weather conditions, such heavy rain or cloudy (RMN, 2003, 2005).

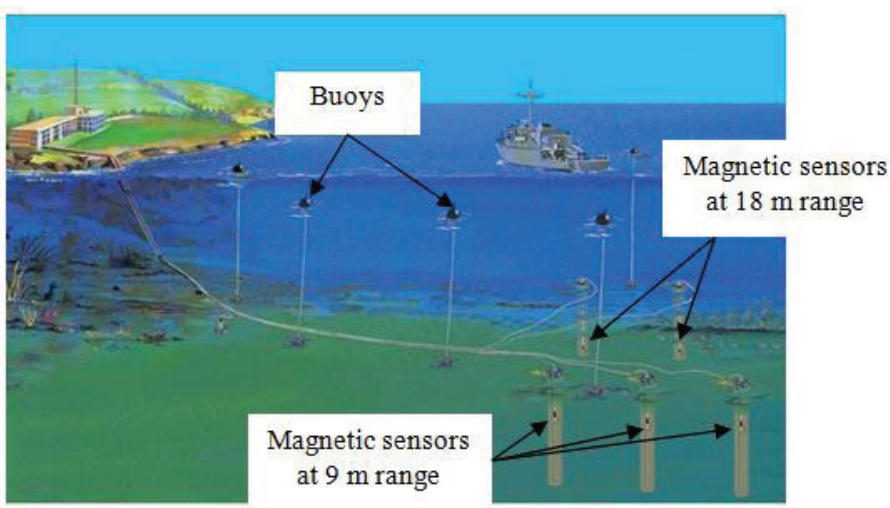

Figure 7:The DG range facility at the Lumut RMN base. (Adapted from RMN (2003))

The major drawback of DG systems is the requirement to monitor changes in the vessel's magnetic source strength and to reoptimisethe compensation system's settings. Once a vessel has been degaussed and leaves the facility, it must monitor and maintain its magnetic level state throughout normal operations. Since a vessel's induced magnetisation changes with its orientation within the earth's local magnetic field, a DG system controller must monitor its location and orientation. Changes in a vessel's permanent magnetisation are the most difficult of the important magnetic field sources to monitor and keep well compensated within a DG system (Holmes, 2008). Frequent ranging of a DG system will prevent the permanent signature from drifting too far astray from specifications. The RMN requires that large vessels, such as frigates, should be degaussed every six months, and every three months for small vessels (RMN, 1986).

3.2 Deperming

All modern vessels, being constructed largely of steel, have permanent magnetic fields surrounding the vessels. Hence, simple induction coils in both older mines and magnetometers in modern mines are equipped to detect magnetic fields surrounding large vessels. Techniques exist to reduce the permanent magnetism of ships through deperming. Most countries typically perform deperming of their vessels by passing large currents through coils temporarily rigged over the exterior of the hull when alongside or docked (Figure 8). Deperming is a one-off treatment, performed once or twice a year that involves altering the permanent magnetism in ships, submarines or other military vehicles (MacBain, 1993). The aim of deperming a vessel is to erase any magnetic history, minimise permanent longitudinal (bow to stern) magnetisation (PLM) and optimise permanent vertical magnetisation (PVM) for the anticipated region of operation. The latter objective involves donating a specific PVM that is designed to counteract the induced vertical magnetisation (IVM) in the relevant magnetic zone of the earth's magnetic field (Figure 9). This will aid the DG coils concerned with minimising vertical magnetisation, and consequently reduce the amount of power required. However, a deperm process, including the preparation, is time consuming, labour intensive and expensive.(Bayneset *et al.,* 2002).

Figure 8: A submarine being depermed at a magnetic treatment facility. (Source: Holmes (2008))

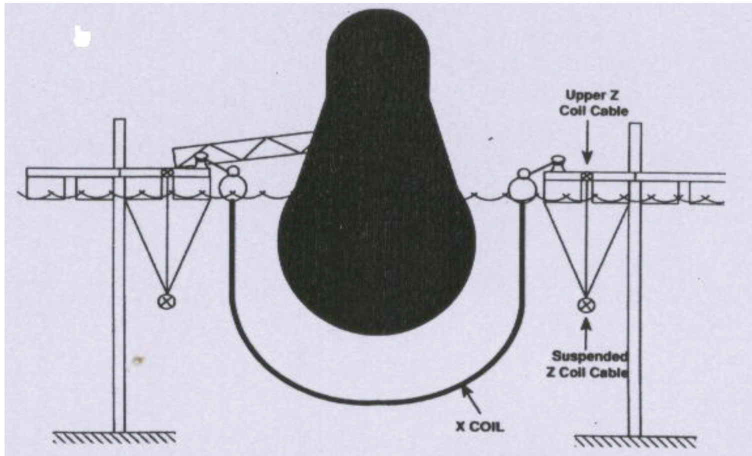

Figure 9: A submarine in a magnetic treatment facility being wrapped with an X coil to minimise PLM. The Z coil cable is used to minimise IVM.
(Source: Baynes *et al.*(2002))

3.3 Shaft Grounding

The presence of underwater SE and AE fields has been known for some time and it has been standard practice in many countries to fit their vessels with passive grounding systems. The system generally consists of a brush and slip ring assembly that connects the shaft directly to the hull of the vessel. It provides for a lower resistance to the ground for current passing through the shaft, thus eliminating some of the variations in resistance as the shaft turns (Figure 10). However, such passive systems do not eliminate all of the variations in the field. Furthermore, brush and slip ring assemblies tend to degrade greatly over time, particularly if maintenance is poor, and as a result, the benefits are lost (Birsan, 2009).

A more effective approach to managing current flow through the shaft of a vessel is through the use of an active shaft grounding (ASG) system (Figure 11). This system uses electronics to compensate for changes in shaft to hull resistance, thereby eliminating the modulation of the shaft current. It operates by using slip-ring sensors to measure the shaft to hull potential of the ship. By determining the variations in the current in the shaft, electronics in the ASG make use of a high current power supply to draw a proportional current through a second slip ring assembly. The ASG device therefore acts as a current bypass for the shaft bearings and seals. The fluctuations in the shaft current are thus eliminated and hence, the AE and AM portions of the electromagnetic signature due to shaft current modulation are eliminated (Thompson *et al.*, 2000)

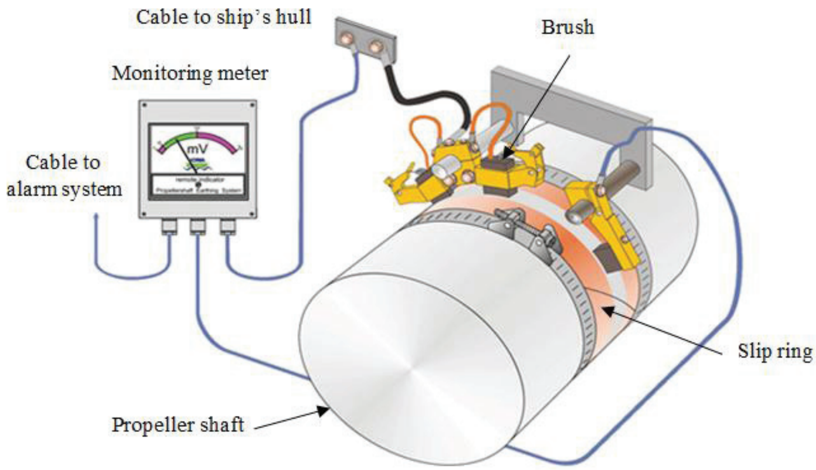

Figure 10: A passive shaft grounding system. (Adapted from Birsan (2009))

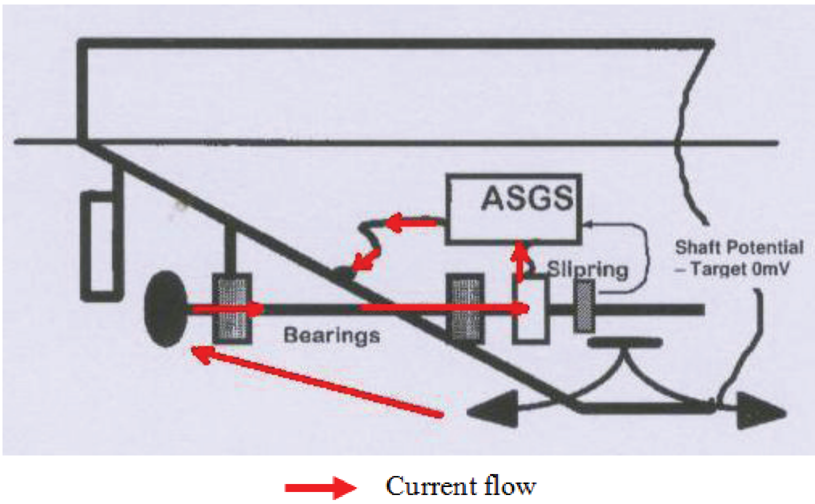

Figure 11: Schematic diagram of an ASG system. (Source: Torrance (2005))

3.4 Active Cathodic Protection (ACP) Design and Filtering

Cathodic protection systems are required by all vessels for the purpose of protecting the hull and appendages from damaging corrosion. Therefore, there is a continuous need for current to flow through the shaft to protect the ship. As a result, it is not feasible to completely eliminate the SE component of the vessels' electromagnetic signature. Methods are however available for reducing SE signatures of vessels. This technique is not applicable to control AE signatures (Kakuba, 2005).

This technique can be applied during ship design and construction in order to minimise the size of the electric dipoles, thus reducing the intensity of the SE field. By carefully determining the optimum placement of the electrode plates on the hull of the vessel, the SE field can be minimised without compromising the corrosion protection of the cathodic protection system (Figure 12). It has also been proposed that by constructing the ship's propeller and other major components solely of electro-chemically equivalent materials, naturally occurring currents that flow between dissimilar metals could be eliminated and hence, there would be no need for an ACP system. Modern metal coatings for steel also help in preventing hull corrosion (Bushman, 2010).

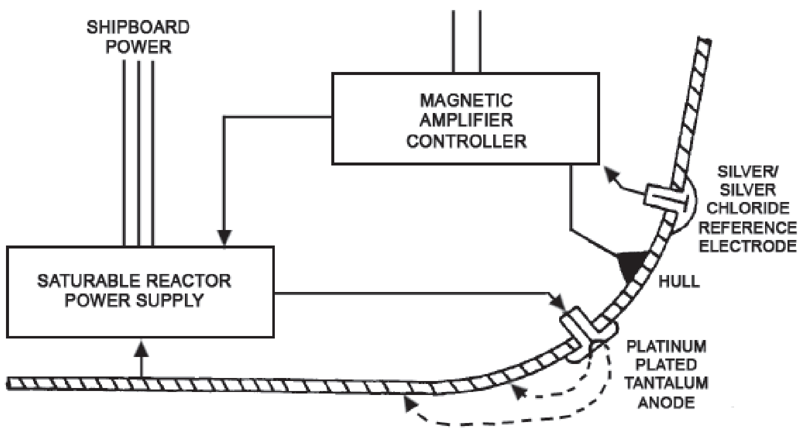

Figure 12: Diagram of location of electrode for an ACP system.
(Source: NAVSEA, 1983)

The system using a high current power supply needs to be filtered appropriately during the cathodic protection process. If the supply is poorly filtered, and the fundamental and harmonic frequencies of the vessel's power system are introduced into the cathodic protection current. This variation can be detected by sea mines or surveillance sensors as part of the vessel's signature. These frequencies can be eliminated from the signature with a passive filter connected to the power supply output. A passive filter is used to protect the power supply by restricting the harmonic current entering the power sources by minimising the effects of harmonic. This will reduce non-required frequencies in the system (Jeffrey & Brooking, 1999).

3.4 Equipment and Cable Wiring Design

In order to reduce SM, SE, AM and AE fields due to stray field sources, such as vessel wiring and rotating machines, the equipment is designed to counter its own radiating fields (i.e. two rotating sources placed next to each other, but in opposite directions), while the ship's wiring is designed to minimise the area between a hot lead and its return conductor (i.e., twisted pairs, return loops for DC feeds being run in the same wireway as the lead loop) (Georgiana & Gheorghe, 2012). Proper up-front design of a power system and its distribution cables can reduce a significant amount of stray fields cheaply and with low impact on the vessel. For example, if two power cables are divided into six or eight separate conducting cables, they can be configured so as to significantly reduce their stray magnetic field signatures (DOD, 1981)

There are many standards that have been produced by defence agencies to counter this problem. For example, the Department of Defence (DOD), US, has produced a few standards, such as DOD-STD-2133 (Cable Arrangement for Minimum Stray Magnetic Field), DOD-STD-2134 (Storage Battery Arrangement for Minimum Stray Magnetic Field) and DOD-STD-2146 (Design of Direct Current Generators and Motors, Low Stray Magnetic Field). The importance of stray field signatures will increase in the near future. Currently, the US Navy is committed to developing all-electric vessels that will use large electric motors for propulsion. As the power supply to electric propulsion motor is a high voltage battery, it would result in very large currents flowing through the vessel's power system, having adverse effect on the vessel's electromagnetics signatures.

3.5 Material Choices for Vessel Construction and Positioning of Equipment

In order reduce SM and AM fields from the earth's magnetic field and / or stray field sources, vessel designers may employ low permeability material in the vessel and / or equipment construction. The use of low permeability materials is common in the design of minesweepers (glass reinforced plastic (GRP), wood and aluminium hulls) and minesweeping equipment (stainless steel and plastic) (Diaz & Tims, 1999).

Equipment containing unavoidable magnetic sources, such as transformers and electric motors, are preferably located as high in the vessel as is practicable and are evenly dispersed through the vessel to avoid producing peaks in the vessel's magnetic signatures. The equipment orientation in the vessel also needs to be emphasised, where long thin objects shall be oriented horizontally to minimise their magnetic fields beneath the vessel (RMN, 2005).

4. CONCLUSION

The electromagnetic field of vessels can be easily exploited by sea mines and hence, steps must be taken to minimise electromagnetic signatures of naval vessels. The SM, SE, AM and AE signatures can be reduced by using systems such as DG, deperming and shaft grounding. In addition, electromagnetic signatures can be minimised through proper design of systems and equipment. Material choices for vessel construction and positioning of equipment in vessels are also important.

Naval vessels should be complemented with the systems and methods discussed above to make them safe and hard to detect by enemies. However, to ensure that vessels are free from the explosive materials, navies also need to be concerned with other vessel signatures, such as acoustic, infrared, wake, pressure and infrared signatures.

REFERENCES

Baynes, T.M., Russell, G.J. & Bailey, A. (2002). *Laboratory Simulation of the Deperm Process*. Defence Science & Technology Organisation (DSTO), Edinburgh, Australia.

Birsan, M. (2008). *Prediction of the Ship's Permanent Magnetization*. Technical Memorandum, Defence R&D Canada, Ottawa, Ontario, Canada.

Birsan,M. (2009). The ELF magnetic field generated by the rotation of the NAB propeller. *6th Int. Conf. Marine Electrom.*, 7-9 July 2009, Stockholm, Sweden.

Birsan, M. (2010).*Measurement and Model Predicted Corrosion Related Magnetic Signature*. Defence R&D Canada, Ottawa, Ontario, Canada.

Bright Hub Engineering (BHE) (2009).*What is Degaussing of Ships?* Available online at: http://www.brighthubengineering.com/marine-engines-machinery /43712 -whatis-degaussing-of-ships/ (Last access date: 24 April 2013).

Bushman, J.B. (2010). *Impressed Current Cathodic Protection System Design*. Bushman & Associates, Inc., Medina, Ohio, US.

Castles, B. (1997). Practical emulation minesweeping.*Sea Tech.*, **21**: 20 – 28.

Changsheng, S.L. (2005). Hidden dragon in the deep: The present situation and development of PLA mine weaponary. *World Outlook*, **9**: 33-40.

Davidson, S.J., Ganderton, C.P., Rawlins, P.G. & Watson, S.M. (1998).*Electric and Magnetic Signatures: Ship Design and Signature Management*. Ultra Electronics PMES Signature Management, UK.

Department of Defense (DOD), US (1981). *DOD -STD-2133: Cable Arrangement for Minimum Stray Magnetic Field.* Department of Defense (DOD), US.

Department of Defense (DOD), US (2007). *Unmanned System Roadmap 2007–2032*. Department of Defense (DOD), US.

Diaz, E.S., Adey, R.A., Baynham, J. & Pei, Y.H. (2001). Optimization of ICCP systems to minimize electric signatures. *Marine Electrom.Conf.*, Stockholm, Sweden.

Georgiana, M. & Gheorghe, S. (2012). Aspects regarding ship magnetism generated by corrosion currents and stray fields. *J. Marine Tech. Environ.*, **1**: 75-80.

Glosny, M. (2004). Strangulation from the sea? *Int. Secur.*,**4**: 125-155.

Hartmann, G.K. & Truver, S.C. (1991). *Weapons that Wait: Mine Warfare in the U.S. Navy*.Naval Institute Press, US.

Hewson, R. (2005). Type 500 and 1000 mines, underwater weapons.*Jane's Air Launched Weapons*,**40**: 98-105.
Holmes, J.J. (2006). *Exploitation of a Ship's Magnetic Field Signatures*. Morgan & Claypool, US.
Holmes, J.J. (2008). *Reduction of a Ship's Magnetic Field Signatures*. Morgan & Claypool, US.
Jeffrey, I.& Brooking, B. (1999). A survey of new electromagnetic stealth technologies. *ANSE 21st Century Combatant Tech. Symp.*, 27-30 January 1998, Biloxi, Mississippi.
Kakuba, G. (2005). *The Impressed Current Cathodic Protection System.*Master Thesis, Department of Mathematics and Computer Science, Eindhoven University of Technology, Netherlands.
Mason, W. (2009). *Naval Mines Technologies*. Briefing presented at Farragut Technical Analysis Centre, Washinton DC.
MacBain, J.A (1993). Some aspects of vehicles degaussing.*IEEE Trans. Mag.*, **29**: 159-165.
McElman, J. (2007). ICCP systems and electromagnetic signatures.*US Navy ICCP Conf.*, 17-18 January 2007, San Diego.
Ministry of Defence (MOD), UK (2008). *DEF STAN 02-612 Issue 2: Guide to the Design of Ferro-magnetic Signature Control System and Degaussing.* Ministry of Defence, UK.
Morison,S. (1995). *Guide to Naval Mine Warfare*. Pasha Publication,US.
Naval Sea System Command (NAVSEA) (1983). *Navals Ships Technical Manual: Chapter 633- Cathodic Protection*. Naval Sea System Command (NAVSEA), US.
Poteete, S. (2010). *Navy's N-Layer Magnetic Model with Application to Naval Magnetic Demining*. Master Thesis, Department of Oceanography, University of Washington, US.
Proshkin, S. (2011). *Russian Seamines*. Gidropribor Central Research Institute, Russia.
Rodrigo, F.J. & Sanchez, A. (1990).*Using Electric Signatures for Extracting Target Navigation Parameters.* Advanced Studies and DSP Technical Area, Sociedad Anonima de Electronica – Submarina (SAES), Spain.
Royal Malaysian Navy (RMN) (1986). *Memo Am Panglima Armada No. 4/86 (1986): Arahan Pelaksanaan Penyahgausan*. Royal Malaysian Navy (RMN), Malaysia.
Royal Malaysian Navy (RMN) (2003). *System Degaussing Range Lumut Instruction Manual*. Royal Malaysian Navy (RMN), Malaysia.
Royal Malaysian Navy (RMN) (2005). *BRL 4010 (2005): Degaussing Manual*. Royal Malaysian Navy (RMN), Malaysia.
Royal Malaysian Navy (RMN) (2011).*Short Courses of Introduction to MR80/B.* Royal Malaysian Navy (RMN), Malaysia.
Diaz, E.S. & Tims, R. (2006).A complete underwater electric and magnetic signature scenario using computational modelling. *Marine Electrom.Conf.*, Amsterdeam, Netherlands.
Thompson, J., Vaitekunas, D. & Brooking, B. (2000). Signature management – the

pursuit of stealth lowering warship signatures: electromagnetic and infrared. *SMi Conf.Signat. Manag*, 21-22 February2000, London, UK.

Torrance,B. (2005). Low signature impressed current cathodic protection – new developments – future concepts. *Underwater DefenceTech Eur.*, Amsterdam, Holland.

Watts, A. (2005). *Jane's Underwater Warfare System 2005-2006*. Jane's Information Group, London.

Defence S&T Tech. Bull., 6(2): 111-129, 2013

BIOWEAPONS AND BIOTERRORISM: A REVIEW OF HISTORY AND BIOLOGICAL AGENTS

Orlando Cenciarelli[1,2*], Silvia Rea[2], Mariachiara Carestia[1], Fabrizio D'Amico[1], Andrea Malizia[1], Carlo Bellecci[1], Pasquale Gaudio[1], Antonio Gucciardino[1] & Roberto Fiorito[3]

[1]Department of Industrial Engineering, Faculty of Engineering
[2]Department of Biology, Faculty of Mathematics, Physics and Natural Sciences
[3]Department of Bio-Medical & Prevention, Faculty of Medicine and Surgery
University of Rome Tor Vergata, Italy

[*]Email: orlando.cenciarelli@uniroma2.it

ABSTRACT

Bioweapons is a thorny issue due their destructive capabilities, and for the potential to generate panic and terror among the affected people. Used since pre-Christian times, bioweapons have resulted in the decimation of whole populations and have changed the geopolitics of several places. In this paper, a summary of the main wars and terrorist activities carried out using bioweapons over the time is presented. In addition, the main biological warfare agents and related pathologies are considered, as according to the U.S. Centers for Disease Control and Prevention's (CDC) priority classification. The emergence of potentially more destructive biological agents, due to the widespread introduction of biotechnology, is also analysed.

Keywords: *Bioweapons; bioterrorism; biological agents and toxins; fatality rates; biosafety level (BSL).*

1. INTRODUCTION

DaSilva (1999) defined biological warfare as the intentional use of microorganisms, and toxins, generally of microbial, plant or animal origin, to produce diseases and deaths among humans, livestock and crops. Biological warfare and bioterrorism are very complex subjects, mainly due to the many agents that can be used as weapons and for the wide range of ways for dissemination into the environment and population. A biological event provides for the presence of at least two actors: one or more pathogens (bacteria, viruses or toxins) and a vehicle for their dissemination. In addition to the high spread capacity and lethality of potential biological agents, their invisibility and extremely difficult short-term detection makes it impossible for immediate diagnosis until the subsequent increase of infections. In fact, most biological weapons (except, for example, toxins and bacterial spores) have a unique quality that other non-conventional weapons (such as chemical and radiological) do not have; biological agents are able to multiply in the host organism and be transmitted in turn to new hosts, generating in this way with unpredictable effects on the population, both in terms of number of victims and geographical spread (Rotz *et al.*, 2002; Zalini, 2010; Vogel, 2012; Tucker, 2013).

Among the reasons which make bioweapons attractive is their very low cost when compared to both conventional and unconventional weapons. For example, NATO (1996) reported that according to data processed in 1969 by U.S. experts, the costs for an attack on an area of 1 km^2 to civilian populations with different weapons are: 1$/$km^2$ for bioweapons, 600$/$km^2$ for chemical, 800$/$km^2$ for nuclear and 2,000$/$km^2$ for conventional armaments. Furthermore, recent advances in life science and biotechnology have made it relatively straightforward to produce large quantities of biological agents with facilities and expertise available to everyone, even to terrorist and paramilitary groups (Zalini, 2010; Vogel, 2012; Tucker, 2013).

In this paper, a summary of the main wars and terrorist activities carried out using bioweapons over the time is presented. In addition, the main biological warfare agents and related pathologies are considered, as according to the U.S. Centers for Disease Control and Prevention's (CDC) priority classification. The emergence of potentially more destructive biological agents, due to the widespread introduction of biotechnology, is also analysed.

2. HISTORY OF BIOLOGICAL WARFARE

2.1 Pre-World Wars

The use of biological agents as war weapons is not a modern era novelty. Although it is not easy to identify a definite time when the use of bioweapons began, ancient evidence reported that in pre-Christian era, around 300 B.C., the Greeks used animal cadavers to contaminate water wells of enemies. This strategy was also used the by the Romans and Persians (SIPRI, 1971a). In a later period, during the battle of Tortona, Italy, in 1155, bodies of dead soldiers and animals were used to contaminate water wells by Emperor Barbarossa's troops (Clarke, 1968). In the 14th century, during the siege of Kaffa by the Tartars (now Feodosiya, Ukraine, a city near the Black Sea, at that time under the control of the Genoese), among the Tartar army, an epidemic of plague was spread. The besiegers thought to catapult the cadavers of their dead comrades within the walls of the city of Kaffa, resulting in a turning point in the war; the Genoese fled from Kaffa, carrying with them their sick. On the return trip to Genoa, they ported at several ports in the Mediterranean Sea. While some sources believe a possible correlation between the epidemic of plague in Kaffa and the pandemic that decimated most of the population of Europe in the following decades (Black Death), most authors share the view of two events were independent (Wheelis, 2002).

In 1422, during the siege of Carolstein, Lithuanian soldiers catapulted cadavers of dead soldiers and excrements into the city, frightening the population affected and spreading lethal fevers in many cases (Newark, 1988). The next documented use of biological agents as a war weapon occurred more than three centuries later. During the French-Indian War (1754-1767), the British commander, Sir Jeffrey Amherst, ordered the distribution of blankets infected with smallpox to decimate the population of Indian tribes hostile to the British. The distribution of infected blankets occurred in the summer of 1763, and the resurgence of the virus among the indigenous lasted for more than 200 years (Bhalla & Warheit, 2004; Riedel, 2004).

2.2 World Wars I and II

Several biological warfare actions carried out during the World War are not sufficiently confirmed in the literature. However, it is frequently reported that the Germans inoculated cattle with *Bacillus anthracis* and *Pseudomonas mallei*, responsible to cause severe diseases such as anthrax and glanders, before sending them into enemy states (SIPRI, 1971a; Poupard and Miller, 1992; Hugh-Jones, 1992). As World War I saw the large-scale use of non-conventional chemical weapons, it was expected that World War II would see more extensive use of biological weapons.

During this war, many countries conducted research programmes on the development of bioweapons; the Japanese programme, conducted under the direction of Lt. Gen. Shiro Ishii, was certainly the most ambitious (1892-1959). The research in this direction started in 1928; during this year, Lt. Gen. Ishii visited many European and American countries to learn useful techniques and information about the possible uses of biological weapons. Upon returning to his homeland, he was provided a substantial grant in order to constitute a massive bioweapons research centre, known as the Unit 731, located at Beiyinhe in Manchuria. The research centre staffed over 3,000 scientists, mainly microbiologists. The experiments were conducted on prisoners of war, principally Koreans, Chinese and Russian soldiers. The prisoners were used to test numerous bioweapons, including *Yersinia pestis*, *Vibrio cholera*, *Neisseria meningitidis* and *Bacillus anthracis* (Leitenberg, 2001). Christopher *et al.* (1997) report that during this research, several thousand prisoners died as a result of the experiments conducted on them. However, the mortality rate around the area of Unit 731 remained very high for several years. If we consider the total count these deaths, we reach the considerable sum of 200,000 deaths as a result of the activities carried out by Lt. Gen. Ishii (Harris, 2002). In 1942, the poor control of the infection spread resulted in the death of 1,700 Japanese soldiers (Sokolski & Ludes, 2001).

Many other nations carried out experiments on potential biological agents, but information reported in the literature is rather limited. It is important to note the experiments conducted in 1942 by the British army on the Island of Gruinard, off the Scotland coast, where anthrax dirty bombs were tested (Manchee *et al.*, 1981).

The island was contaminated and uninhabitable until 1990, when extensive land decontamination was carried out (Aldhous, 1990).

2.3 Post-World Wars

Until World War II, the U.S. remained considerably behind other nations in research on bioweapons. The golden age for both the test and development of bioweapons in the U.S. was immediately after the conclusion of World War II, when it received the results of the experiments performed by the Japanese Unit 731. The U.S. also worked directly with Lt. Gen. Ishii, the former director of Unit 731 (Christopher *et al.*, 1997).

In September 1950, the U.S. Navy conducted an experiment on civilians in order to assess the vulnerability of a large American coastal town to a biological attack; in the San Francisco Bay, a cloud of *Serratia marcescens* (a low pathogenic bacterium mainly responsible for infections of skin and respiratory tract) was spread by boat. The infection struck, as a result of subsequent checks, almost the entire population (1 million people). Even though the bacterium was almost harmless, several individuals showed effects of respiratory diseases and some of them died (Christopher *et al.*, 1997).

A few years later (1956-1958), in Georgia and Florida, swarms of mosquitoes, probably carriers of yellow fever, were released in order to verify vulnerability to an air attack. Even though the documents are still kept top secret, several sources report that some individuals died from the bites of insects. A last large scale experiment which was documented, consists of the dissemination of *Bacillus subtilis* in the New York subway in the summer of 1966. The experiment resulted in the infections, although without consequences, of more than one million people. It demonstrated that the spread of a pathogen in the whole subway network from a single station, due to the displacement of air in the tunnels, was possible (Zygmunt, 2006).

In the 1970s, the USSR conducted an ambitious research programme on bioweapons, but, unlike the U.S. programmes, of which the secrecy has been partially removed, an aura of mystery about Russian research programmes still remains. According to Davis (1999), the USSR, between 1973 and 1974, formed an organisation called the Chief Directorate for Biological Preparation (Biopreparat), with the purpose of developing and producing bioweapons. Although there are no unambiguous data about the number of individuals employed by Biopreparat, it is believed that more than 50,000 people were working in the whole system connected to the structure, including scientists and technicians, who were placed in 52 research and production factories. In these facilities, high amounts of etiologic agents of plague, tularemia, anthrax, glanders, smallpox and Venezuelan equine encephalomyelitis were studied and produced. In addition to biological agents from natural sources, the Soviets also studied and applied technologies of genetic engineering in order to increase the aggressiveness of biological agents through biotechnology The aim of this work was the production of a new more dangerous, more easily spread and more difficult to identify combat generation of bioweapons.

Among the countries that developed a massive programme on bioweapons research, in the post-World Wars era, is Iraq. It started its research and development programme in the field of biological warfare in 1974, contextualising it in an organisation called the State Organization for Trade and Industry (Davis, 1999). The programme consisted of the study and production of botulinum toxin, anthrax, aflatoxin and ricin, as well as antiplants and viral agents, such as rotavirus, infectious hemorrhagic conjunctivitis and camel pox. The programme involved about 300 scientists, who completed their training in Western European countries (Leitenberg, 2001).

2.4 International Treaties

The first measures against the use of bioweapons were taken in the 19th century during the Hague Conference in 1899, and then confirmed in the same place in 1907, with the document entitled *Laws and Customs of War on Land*, signed and ratified by 24 countries regarding the prohibition on the use of poisoned arms (Leitenberg, 2001). In 1925, with awareness of the horrors of World War I, especially in regards to the use of chemical weapons, the Geneva Protocol on the *Prohibited Use in War of Asphyxiating, Poisonous or Other Gases, and of Bacteriological Methods of Warfare* was signed.. Although this treaty was signed by a considerable number of nations (even though it was only ratified by the U.S. in the mid-1970s), it only prohibited the use of biological agents as weapons, but not their development and stockpiling (Christopher *et al.*, 1997).

In view of the limited effectiveness of the Geneva Protocol in the control of bioweapons development and proliferation, in 1972, the *Convention on the Prohibition of the Development, Production and Stockpiling of Bacteriological (Biological) and Toxin Weapons and on Their Destruction* was initiated. Initially signed by over 100 nations, the Convention became effective in 1975. However, this convention, similar to the Geneva Protocol, has several loopholes. First of all, it does not provide guidelines for the protocol on compliance verification. Moreover, it only prohibits the use and development of bioweapons in quantities that have no justification for prophylactic, protective or other peaceful purposes (Riedel, 2004). It is evident how this assertion is open to interpretation, as it does not define the threshold quantities or substantial limitations to the development and production of bioweapons (SIPRI 1971b, 1973). Bioterrorist events that have taken place consequent to the ratification of the Biological Weapons Convention (BWC) in 1972 have confirmed that the convention does not prevent the proliferation of biological weapons.

2.5 The Rise of Bioterrorism

Even after the ratification of the BWC, a large number of countries went on to develop, produce and test biological agents for military purposes. Since the 1980s, terrorist groups have increasingly considered bioweapons as a highly destabilising tool for civil society and economy. The large scale advent of biotechnology and the reduced difficulty in production of genetically modified organisms have made the potential creation of multi-drug resistant pathogens with enhanced virulence factors possible. The use of biological agents in the last decades is mainly attributable to terrorist groups, more or less isolated, who used bioweapons as a strategy to defend extremist religious ideas by striking civilian populations or sensible government targets (Cronin, 2004).

In 1984, in The Dalles, Oregon, U.S., a group of extremist followers of Bhagwan Shree Rajneesh (also known as Osho) contaminated the salad in 10 different salad bars with the pathogen of salmonellosis, *Salmonella thyphimurium*, in order to disable the population. A total of 751 people contracted the disease and several of them were hospitalised. Although there were no fatalities, this terrorist act is considered the largest bioterrorist attack in the history of the U.S. (Török *et al.*, 1997). In the 1990s, the Japanese cult of Aum Shinrikyo tested different bioweapons, including botulin toxin, anthrax, cholera, and Q fever. In 1993, during a humanitarian mission in Africa, it tried to obtain samples of the Ebola virus. Between 1990 and 1995, the cult attempted to carry out several bioterrorist acts in Tokyo using vaporised biological agents, including botulinum toxin and anthrax spores. Fortunately, the attacks were unsuccessful (Olson, 1999).

A significant bioterrorist event occurred in the U.S. contextually to the dramatic attacks to the World Trade Center in New York in September 2001. The release of *Bacillus anthracis* spores through the U.S. postal system was carried out with letters addressed to the press and to government officials. There were 22 confirmed cases of anthrax contamination, consisting of 12 cutaneous and 10 inhalational cases. The 12 cutaneous patients responded positively to antibiotic treatment, while of the 10 inhalational cases, 4 were fatal (McCarthy, 2001). In 2002, in Manchester, U.K., six terrorists were arrested for being found in possession of ricin, and in 2004, traces of the same toxin were found at the Dirksen Senate Office Building in Washington D.C. (Bhalla & Warheit, 2004) It appears evident then that the use of biological agents has moved, in recent times, to terrorist groups. This creates very strong concerns that the use of bioweapons by terrorists can create unexpected scenarios characterised by massive destructive potential.

3. BIOLOGICAL AGENTS

3.1 Categories of Biological Agents

The U.S. Centers for Disease Control and Prevention (CDC) defines a bioterrorism attack as "*the deliberate release of viruses, bacteria or other germs (agents) used to cause illness or death in people, animals, or plants*" (CDC, 2013). It classifies biological agents into three categories (Table 1):

1. Category A: Agents that can be easily disseminated or transmitted from person to person. They result in high mortality rates and have the potential for major public health impact. They might cause public panic and social disruption, and require special action for public health preparedness.

2. Category B: Agents that are moderately easy to disseminate. They result in moderate morbidity rates and low mortality, and require specific enhanced diagnostic capacity and disease surveillance.

3. Category C: Emerging agents that could be engineered for mass dissemination in the future because of their availability. They are easy to produce and disseminate. They are potentially linked to high morbidity and mortality rates, and major health impact.

Generally, biological agents (included those used as bioweapons) can be further classified according to certain characteristics that define the hazard to health (NATO, 1996):

a. Infectivity: The aptitude of an agent to penetrate and multiply in the host.
b. Pathogenicity: The ability of the agent to cause a disease after penetrating into the body.
c. Transmissibility: The ability of the agent to be transmitted from an infected individual to a healthy one
d. Ability to neutralise: Its means to have preventive tools and / or therapeutic purposes.

Biological agents can be transmitted through one or more ways. The transmission modes are the following (La Placa, 2010):

a. Parenteral: Agents that are transmitted through body fluids or blood.
b. Airway (by droplets): Agents that are emitted by infected people, which can then be inhaled by surrounding people.
c. Contact: Through which the agents present on the surface of the infected organism can infect another organism.
d. Oral-faecal route: Through objects, foods or other items contaminated with the faeces of infected patients, or through sexual contact.

Table 1: Major biological agents that are possible to be used as bioweapons (CDC, 2013).

Groups	Diseases	Agents
A	Anthrax	*Bacillus anthracis*
	Botulism	*Clostridium botulinum* toxin
	Plague	*Yersinia pestis*
	Smallpox	*Variola major*
	Tularemia	*Francisella tularensis*
	Viral hemorrhagic fevers	*Filoviruses and Arenaviruses*
B	Brucellosis	*Brucella spp.*
	Epsilon toxin	*Clostridium perfringens*
	Food safety threats	*Salmonella* spp., *E.coli* O157:H7, *Shigella*
	Glanders	*Burkholderia mallei*
	Melioidosis	*Burkholderia pseudomallei*
	Psittacosis	*Chlamydia psittaci*
	Q fever	*Coxiella burnetii*
	Ricin toxin	*Ricinus communis*
	Staphylococcal enterotoxin B	*Staphylococcus spp.*
	Typhus fever	*Rickettsia prowazekii*
	Viral encephalitis	*Alphaviruses*
	Water safety threats	*Vibrio cholerae*, *Cryptosporidium parvum*
C	Emerging infectious diseases	*Nipahvirus* and *Hantavirus*

3.2 Biological Agents That Can Be Used as Bioweapons

While there are numerous pathogens (bacteria, viruses and toxins) that cause diseases in humans, animals and plants, only very few possess the characteristics to be a bioweapon. Eitzen (1997) described the characteristics that make a biological agent a potential bioweapon. Ideally, a bioweapon should be easy to find or produce. In order to develop a biological attack towards sensitive targets or the population, large amounts of biological agents are in fact required; it must be considered that it is necessary to have quite a number of biological agents (or a certain amount of toxin) to generate a disease in a target. The ideal bioweapon also must have a high capacity to incapacitate the affected or, alternatively, be highly lethal. It is appropriate to choose an agent with an incubation period depending on whether immediate or delayed effects are required. Other important characteristics for a biological weapon are the route of transmission, and hence, the ease of dissemination with an appropriate method of delivery. Finally, the stability of the agent must be assessed, especially when large quantities must be stored for indefinite periods (Kortepeter & Parker, 1999).

In the following sub-sections, the key features of the most relevant biological agents (included in category A by the CDC) are reported and categorised according to biological origin. The fatality rates of these agents are shown in Table 2, while the biosafety levels (BSL) required to work with the respective agents are shown in Table 3.

Table 2: Fatality rates of Category A biological agents.

Pathogen	Biological Agent	Fatality rate (%)	Reference
Bacteria	*Bacillus anthracis*	Cutaneous: <1% Respiratory: 75% Gastrointestinal: 25%-60%	CDC, 2013
	Clostridium botulinum	Foodborne: 3-5% Wound and intestinal: 15%	
	Yersinia pestis	8-10%	WHO, 2004
	Francisella tularensis	Subspecies *tularensis*: 2%	WHO, 2007; Dennis *et al.*, 2001
		Subspecies *holarctica*: fatal cases are rare	WHO, 2007
Virus	*Variola major*	30%	CDC, 2013
	Filoviridae	90%	Warfield *et al.*, 2005
	Arenaviridae	15-30%	Briease *et al.*, 2009

Table 3: Biosafety levels (BSL) required to work with Category A biological agents.

Pathogen	Biological Agent	BSL	Reference
Bacteria	*Bacillus anthracis*	3	WHO, 2004
	Clostridium botulinum	3	Arnon *et al.*, 2001
	Yersinia pestis	2-3	WHO, 2004
	Francisella tularensis	3	Bhalla & Warheit, 2004
Virus	*Variola major*	4	DHHS, 2009
	Filoviridae	4	
	Arenaviridae	2-3	

3.2.1 Bacteria

3.2.1.1 *Bacillus anthracis*

Bacillus anthracis is a Gram-positive, non-motile, facultative anaerobic endospore forming bacteria, usually surrounded by a capsule. It is the etiological agent of anthrax, which occurs most frequently when an epizootic or enzootic of herbivores becomes infected after acquiring spores from direct contact with contaminated soil. In humans, the disease can occur when exposed to infected animals, tissue from infected animals or high concentrations of anthrax spores. Anthrax endospores have no measurable metabolism, do not divide, and are resistant to drying, heat, ultraviolet and ionising radiation, chemical disinfectant, and other forms of stress, remaining in the environment for years (Bhalla & Warheit, 2004), with survival in soil for up 200 years being reported (Yuen, 2001).

The disease is caused by the action of a toxin produced by the vegetative bacillus, which consists of three components; protective antigen (PA), edema factor (EF) and lethal factor (LF). PA binds to cell receptors, mediating the entry of EF and LF into the cell. Another anthrax virulence factor is the D-glutamic acid polypeptide capsule of the vegetative form (WHO, 2004). Three types of anthrax infections can occur; cutaneous, inhalation and gastro intestinal. The cutaneous form is the most common and is characterised by dermal ulcers, painless, non-scarring, pruritic papule progressing to a black depressed eschar with swelling of adjacent lymph glands and oedema (WHO, 2004). Local lymphadenitis and fever can occur, but septicaemia is rare (Moquin & Moquin, 2002). Untreated cutaneous anthrax can become systemic and it is fatal in 5-20% of cases. Gastro-intestinal and inhalation forms are less common. The inhalation form starts with influenza-like symptoms that include fever, fatigue, chills, non-productive cough, vomiting, sweats, myalgia, dyspnoea, confusion, headache and chest and / or abdominal pain, followed by the development of cyanosis, shock, coma and death. The gastro-intestinal form is characterised by fever, nausea, vomiting, abdominal pain and bloody stools. Oropharyngeal infection, on the other hand, is accompanied by oedematous swelling of the neck, often followed by fever and lymphoid involvement (WHO, 2004).

There is no evidence of direct person-to-person spread (Yuen, 2001). After exposure, the incubation period is reported to range from 1 to 7 days, possibly extending up to several weeks. Some vaccines are administered to prevent the disease, such as live spore vaccines based on attenuated strains, and cell-free vaccines based on anthrax PA (WHO, 2004). Regarding therapy, there are three types of antibiotics that are effective against *B. anthracis*; ciprofloxacin, tetracyclines and penicillins (Bhalla & Warheit, 2004). For laboratory diagnosis and research, manipulations involving clinical specimens, Biosafety Level 2 (BSL-2) practices are recommended, while for manipulations involving activities with a significant aerosol production, Biosafety Level 3 (BSL-3) practices are advised (WHO, 2004).

3.2.1.2 Clostridium botulinum

Clostridium botulinum is a spore forming and obligate anaerobe, etiological agent of botulism, which can be isolated from the soil, its natural habitat. Four species of *C. botulinum* are known, characterised by different genomes and their common botulinum toxin. In addition, seven distinct antigenic types of botulinum toxin (A-G) are defined by the absence of cross-neutralisation. The toxin is responsible for the disease and is a dichain polypeptide: a heavy chain of 100 KDa is joined by a single disulfide bond to a 50 KDa light chain, which is zinc containing endopeptidase that blocks acetylcholine-containing vesicles from fusing with the terminal membrane of the motor neuron, resulting in flaccid muscle paralysis (Arnon *et al.*, 2001). Botulinum toxin is the most lethal toxin known and all seven types act in similar ways. Death often occurs as a result of paralysis of pharyngeal and diaphragmatic muscles, followed by respiratory arrest (Bhalla & Warheit, 2004).

Three forms of human botulism exist; food-borne, wound and intestinal. All forms of botulism are caused by absorption of botulinum toxin into the circulation from a wound or mucosal surface; after infection, the incubation period depends on the rate and amount of toxin absorption: from two hours to eight days. Patients affected by botulism are febrile and present symmetric, descending flaccid paralysis with prominent bulbar palsies. Therapy consists of passive immunisation with equine antitoxin, accompanied by supportive care. Botulism can be prevented by administration of a pentavalent (ABCDE) botulinum toxoid, which a recombinant vaccine is in development. BSL-2 practices are recommended for manipulations in laboratory, while BSL-3 practices are suggested for activities with high potential for aerosol or droplet production (Arnon *et al.*, 2001).

3.2.1.3 *Yersinia pestis*

Yersinia pestis is a Gram-negative non-motile, non-spore forming coccobacillus that grows both in aerobic and anaerobic conditions. It can remain viable for days in moist soil or water, but it is killed by direct exposure to sunlight (WHO, 2004). The bacterium is the etiological agent of plague, a disease that can affect humans and animals (La Placa, 2010). Wild rodents are the pathogen carriers and transmission to other animals occurs through fleas, infected animal tissues, contaminated soil or respiratory droplet exposures. In endemic rural areas, persons who come in contact with wild rodent hosts of *Y. pestis* can be affected by the plague, which exists in two forms; bubonic and pneumonic plagues (WHO, 2004).

Bubonic plague occurs if fleas are used as carriers of disease, in which the incubation period is 2-6 days after exposure. Swelling of the lymph nodes occurs (bubones) occurs, associated with onset of fever, chills, headache, followed by nausea and vomiting. Untreated bubonic plague causes septicemia. Pneumonic plague can occur from inhaling organisms or from exposure to infected blood. Productive cough with blood-tinged sputum is a typical symptom of pneumonic plague, which can spread from person to person by coughing (La Placa, 2010).

If started soon after infection, antimicrobial therapy is effective. It consists of administration of streptomycin or gentamicin. Alternative antimicrobial substances are tetracyclines, doxycyclines, chloramphenicol, fluoroquinolones, ciprofloxacin and sulfonamides. Plague vaccine is advised only for high-risk groups, such as laboratory personnel. Vaccination with killed or live attenuated *Y. pestis* is effective against bubonic plague but not against pneumonic plague. BSL-2 practices are recommended for activities involving infective materials and cultures, while BSL-3 may be used in the case of high production of infectious aerosol or direct contact with infected fleas (WHO, 2004).

3.2.1.4 *Francisella tularensis*

Francisella tularensis is a small, Gram-negative, non-motile, facultative intracellular, aerobic coccobacillus. It is responsible of tularemia, which is a zoonotic disease. Two bacterium sub-species exist; *F. tulariensis tulariensis* (Type A) and *F. tularensis palaearctica* (Type B). Type A is more virulent than Type B (WHO, 2004). The organism can survive for up to several weeks in soil, water, straw and soil. Many wild animals (rabbits, beavers, muskrats, hares, voles) are the pathogen carriers. Humans can be infected when bitten by arthropods, by ingestion of contaminated food and water, and inhalation of contaminated aerosols. Direct contact with infected animals is also dangerous for humans, but person-to-person transmission has not been observed (Bhalla & Warheit, 2004).

After infection, the incubation period is generally 3-5 days, but it can extend up to 14 days. Symptoms of the disease depend on the virulence of the infectious agent. Two different clinical manifestations exist; ulceroglandular (75% of cases) and typhoidal (25% of cases) tularemia. The first is characterised by indolent ulcer at the site of entry and painful swelling of local lymph glands; the expression “typhoidal tularemia” indicates systemic illness without apparent site of primary infection. Painful pharyngitis and cervical lymphadenitis are caused by infection through ingestion of contaminated food or water (Bhalla & Warheit, 2004).

Treatment consists of administration of intramuscular streptomycin. Parenteral gentamicin can be used as an alternative drug, while for pre-exposure prophylaxis, a live, attenuated vaccine is available. However, for antimicrobial prophylaxis, oral administration of doxocycline or ciprofloxacin is advised for a 14-day period following the last day of exposure. BSL-2 practices are recommended for routine manipulations of clinical specimens from human and animals, while BSL-3 practices are recommended for manipulations including risk of infectious aerosol production (Bhalla & Warheit, 2004).

3.2.2 Virus

3.3.2.1 *Variola major and Poxviridae*

Poxviridae comprise a family of genetically related, large, enveloped, DNA viruses that replicate exclusively within the cytoplasm of vertebrate or invertebrate cells. Only the member of the genus *Orthopoxvirus*, which includes *smallpox*, *monkeypox*, *vaccinia*, and *cowpox* can infect humans. Of these, only smallpox is readily transmitted from person to person via saliva or nasal secretion droplets and contaminated objects (Moss, 2007).

The most common clinicopathologic presentation of smallpox was a systemically virulent form of the disease known as *variola major* with a case mortality rate of up to 30 to 40%. Saliva or nasal secretion droplets from infected individual are responsible of inter-human transmission. After oropharyngeal or respiratory mucosa infection, and the asymptomatic, non-infectiuous period of incubation (7-17 days), many patients present high fever and the malaise of prodromal illness. Maculopapular rashes then appears on the mucosa of the mouth and pharynx, face, and forearms, and spreads to the trunk and legs. This is the most contagious stage because of the high viral titers present in the oropharyngeal tissues. Within 1-2 days, that rash becomes vesicular and later pustular. Scabs subsequently develop that, if the person survives, leave pitted scars called pocks from which the word pox has been derived (Knipe *et al.*, 2001).

A more severe but much less common manifestation of *variola major*, known as malignant or hemorrhagic smallpox, is associated with a near 100% case fatality rate. Humans are the only known hosts of the virus, facilitating the global *Variola* eradication, by the World Health Organization (WHO) in 1980 after a successful global vaccination campaign, which was subsequently discontinued (Fenner *et al.*, 2007). The cessation of vaccination not only exposed populations to the risk of a bioterrorist attacks, but also increasing prevalence of zoonotic *poxvirus* such as *monkeypox* (Rimoin *et al.*, 2010).

Currently, there are no available treatments for smallpox infection and the therapy involves supportive care as antipyretic and anti-inflammatory treatments to relieve pain and fever. Antibiotics are prescribed for eventual bacterial super-infections (Knipe *et al.*, 2001; Bhalla & Warheit, 2004). All experiments using live variola virus are to be done within WHO approved Biosafety Level 4 (BSL-4) laboratories; one is at the CDC in Atlanta, U.S., while the other one is at the State Research Center of Virology and Biotechnology in Koltsovo, Russia (DHHS, 2009).

3.3.2.2 *Filoviridae.*

The *Filoviridae* family (from the Latin term *filum,* referring to shape of the virion), consists of enveloped, negative-stranded, RNA viruses that cause severe zoonotic hemorrhagic fever in humans and non-human primates. The family includes two distinct genera; *Marburgvirus* and *Ebolavirus.* The genus *Marburgvirus* includes a single species, *Marburg marburgvirus*, which has two members, Marburg (MARV) and Ravn (RAVV) viruses. The genus *Ebolavirus* includes five species, each of which has a single member; *Zaire ebolavirus* (EBOV), *Sudan ebolavirus* (SUDV), *Taï Forest ebolavirus* (TAFV), *Bundibugyo ebolavirus* (BDBV) and *Reston ebolavirus* (RESTV) (Adams & Carstens, 2012).

The natural carrier hosts of these viruses have not yet been identified. However, Ebola virus RNA has been detected in terrestrial mammals in Central Africa. Evidence is emerging that African, Asian and possibly also European bats are natural carries of filoviruses and these animals could transmit the virus directly to humans or via intermediate hosts, including gorillas and swine. Following transmission to humans, spread of the virus between individuals is the result of direct contact with blood or other body fluids from infected patients. Filoviruses exhibit different virulence in humans; EBOV and MARV infection is associated with case-fatality rates of up to 90% while RESTV seems to be apathogenic (Sanchez *et al.*, 2007; Kuhn *et al.*, 2011).

In infected individuals, after the incubation period, ranging from 2 to 21 days, the onset of illness begins with generic flu-like symptoms characterised by high fever, severe headache and malaise followed by gastrointestinal symptoms including abdominal pain, severe nausea, vomiting and watery diarrhea.

The majority of patients also present clear hemorrhagic manifestations, such as ecchymoses, mucosal bleeding and hematemesis. Fatalities typically occur 8–16 days following the onset of symptoms, with death usually caused by severe diffuse coagulopathy, multiorgan failure, shock and coma (Brauburger *et al.*, 2012). There is no a specific therapy against filoviral infections and supportive care is provided to limit the symptoms (Clark *et al.*, 2012). Due to the lack of approved therapeutics or vaccines along with the high lethality and infectivity, work with *Filoviridae* is restricted to high-containment BSL-4 laboratories (DHHS, 2009).

3.2.2.3 *Arenaviridae*

Arenaviridae family consists of enveloped, negative-stranded, bi-partite RNA viruses that cause chronic infections in rodents (animals) and zoonotically acquired disease in humans (Salvato *et al.*, 2011). The genus *Arenavirus* includes 22 viral species which, based on genetic and geographical data are divided into two groups; Old World (OW) and New World (NW) complexes. The OW complex includes the world-wide distributed Lymphocytic choriomeningitis virus (LCMV), which causes acute aseptic meningocephalitis in humans, and other viruses endemic to the African continent, including Lassa (LASV) and Lujo (LUJV) viruses, which cause hemorrhagic fever (HF). The larger group of NW arenavirus is further divided into three clades; A, B and C. Clade B is the more relevant in term of human pathology, since it contains most of HF-causing arenaviruses in South America (Charrel & de Lamballerie, 2003).

Virus transmission occurs usually through human contact with excretions or materials contaminated with the excretions of an infected rodent, while secondary person-to-person transmission can occur with some arenaviruses, such as Lassa, Machupo and Lujo viruses (Weber & Rutala, 2001). After 1-2 weeks of incubation period, HF infection produces a wide range of symptoms and pathology, including headache, cough and sore throat, nausea, vomiting, and diarrhea. Several complications can arise, including pleural effusions, neurological complications, facial edema and bleeding from mucosal surface. Advanced stages of disease are often associated with shock and death (Schattner *et al*., 2013). No licensed vaccines, prophylactic or therapeutic treatments are available against arenavirus infection. Currently, therapy consists of ribavirin administration, accompanied by supportive care (Vela, 2012). BSL-4 containment is required for all pathogenic hemorrhagic fever-causing arenaviruses while BSL-2 / 3 laboratory environment is advised for handling of other arenaviruses (DHHS, 2009).

4. CONCLUSION

The use of biological agents as bioweapons has its roots in ancient times, when the concepts of bacteria, toxin or virus were not known yet. Over 2,000 years ago, rudimentary techniques of biological warfare resolved the first disputes among people. Hand by hand with the evolution of modern science (especially in the 18th century), the possibility of using biological agents as bioweapons has been refined. In the last few decades, the development of innovative biotechnology techniques has provided the knowledge to create more aggressive bioweapons. These new organisms cause great concern, because they can produce devastating and completely unexpected effects, of the same level or even higher than the most dangerous wild type biological agents.

Although international conventions prohibit the use of biological agents for offensive purposes, it is known that many terrorist groups continue their research about the possible use of biological agents as bioweapons. The concerns related to biological agents are aroused, as well as the effects in terms of victims, both from the objective difficulties in the detection of a potential attack. A release of biological agents is difficult to detect with current technology, especially when it comes to a stand-off revelation compared to point detection. Biological agents have a unique feature when compared to other non-conventional weapons (chemical or radiological); with the exception of toxins, they are able to multiply in the host and in turn be transmitted to other individuals. Hence, immediate identification of a biological attack is essential, in order to take appropriate containment measures to contain further dissemination. Therefore, there is a clear need to develop new technologies to detect biological agents from long-range, in order to take immediate action in the event of both intentional and unintentional biological agents releases.

ACKNOWLEDGMENT

The authors are very grateful to Dr. Luca Parca, PhD (EMBL, Heidelberg, Germany), Dr. Luca Persichetti, PhD (ETH, Zurich, Switzerland) and Dr. Matteo Vietri Rudan (UCL, London, United Kingdom) for their help in obtaining of bibliographic material and to Adriana Savastano for the critical reviewing of the paper.

REFERENCES

Acheson, N.H. (2011). *Fundamentals of Molecular Virology.* Wiley, New York.

Adams, M.J. & Carstens, E.B. (2012). Ratification vote on taxonomic proposals to the International Committee on Taxonomy of Viruses. *Arch. Virol.* **157**:1411–1422.

Aldhous P. (1990). Biological warfare: Gruinard Island handed back. *Nature,* **344**:801.

Arnon, S.S., Schechter, R., Inglesby, T.V., Henderson, D.A., Bartlett, J.G., Ascher, M.S., Eitzen, E., Fine, A.D., Hauer, J., Layton, M., Lillibridge, S., Osterholm, M.T., O'Toole, T., Parker, G., Perl, T.M., Russell, P.K., Swerdlow, D.L. & Tonat, K. (2001). Botulinum toxin as a biological weapon: medical and public health management. *JAMA*, **285**:1059-1070.

Bente, D., Gren, J., Strong, J.E. & Feldmann, H. (2009). Disease modeling for Ebola and Marburg viruses. *Dis. Model. Mech.* **2**:12-17.

Bhalla, D.K. & Warheit, D.B. (2004). Biological agents with potential for misuse: a historical perspective and defensive measures. *Toxicol Appl Pharmacol.,* **199**:71-84.

Bhalla, D.K. & Warheith, D.B. (2004). Biological agents with potential for misuse: ahistorical perspective and defense measures. *Toxicol. Appl. Pharm.,* **199**:71-84.

Brauburger, K., Hume, A.J., Mühlberger, E. & Olejnik, J. (2012). Forty-five years of Marburg virus research. *Viruses*, **4**:1878-1927.

Buchmeier, M.J., de la Torre J.-C. & Peters C.J. (2007). Arenaviridae: The Viruses and Their Replication. *In:* Knipe D.M. and Howley P.M. (Eds.), *Fields Virology*. Lippincott Williams & Wilkins, Philadelphia, PA, USA, pp. 1791–1827.

Briese, T., Paweska, J.T., McMullan, L.K., Hutchison, S.K., Street, C., Palacios, G., Khristova, M.L., Weyer, J., Swanepoel, R., Egholm, M., Nichol, S.T. & Lipkin, W.I. (2009). Genetic detection and characterization of Lujo virus, a new hemorrhagic fever-associated arenavirus from southern Africa. *PLoS Pathog.* **5**: e1000455.

Burri, D.J., da Palma, J.R., Kunz, S. & Pasquato A. (2012). Envelope glycoprotein of arenaviruses. *Viruses*, **17**: 2162-2181.

Centers for Diseases Control and Prevention (CDC). *Bioterrorism Agents / Diseases*. Available online at: http://www.bt.cdc.gov/agent/agentlist-category.asp (Last access date: 8 September 2013).

Charrel, R.N. & de Lamballerie, X. (2003). Arenaviruses other than Lassa virus. *Antiviral Res.*, **57**: 89-100.

Christopher, G.W., Cieslak, T.J., Pavlin J.A. & Eitzen, E.M. (1997). Biological warfare: a historical perspective. *JAMA*, **278**: 412-417.

Clark, D.V., Jahrling, P.B. & Lawler, J.V. (2012). Clinical management of filovirus-infected patients. *Viruses*, **4**:1668-1686.

Clarke, R. (1968). *The Silent Weapons*. David McKay Co. New York.

Cronin, A.K. (2004). Terrorist motivations for chemical and biological weapons use: Placing the threat in context. *Defense Secur. Anal.*, **20**:313-320.

DaSilva, E. (1999). Biological warfare, bioterrorism, biodefence and toxin weapons convention. *EJB*, **2**:99-129.

Davis, C.J. (1999). Nuclear blindness: An overview of the biological weapons programs of the former Soviet Union and Iraq. *Emerg. Infect. Dis.,* **5**: 509-512.

Dembek, Z.F. (2006). The history and threat of biological weapons and bioterrorism. *In* McIsaac J.H. (ed.), *Hospital Preparation for Bioterror: A Medical and Biomedical Systems Approach.* Elsevier, London.

Dennis, D.T., Inglesby, T.V., Henderson, D.A., Bartlett, J.G., Ascher, M.S., Eitzen, E., Fine, A.D., Friedlander, A.M., Hauer, J., Layton, M., Lillibridge, S.R., McDade, J.E., Osterholm, M.T., O'Toole, T., Parker, G., Perl, T.M., Russell, P.K. & Tonat, K. (2001). Tularemia as a biological weapon – Medical and public health management. *JAMA*, **285**: 2763–2773.

Department of Health and Human Services (DHHS) (2009). *Biosafety in Microbiological and Biomedical Laboratories, 5th ed.* U.S. Department of Health and Human Services (DHHS), Washington, D.C.

Department of Health and Human Services (DHHS) (2010). *Ebola Hemorrhagic Fever Information Packet.* U.S. Department of Health and Human Services (DHHS), Washington, D.C.

Eitzen, E.M. (1997). Use of biological weapons. *In* Zajtchuk, R. & Bellamy, R.F. (Eds.), *Textbook of Military Medicine: Medical Aspects of Chemical and Biological Warfare*. Office of the Surgeon General. U.S. Department of the Army, Washington. D.C., pp. 437-450.

Fenner, F., Henderson, D.A., Jezek, A. & Ladnyi, I.D. (2007) *Smallpox and Its Eradication.* World Health Organization (WHO), Geneva, Switzerland.

Harris, S. (2002). *Factories of Death: Japanese Biological Warfare, 1932-1945, and the American Cover-Up*. Routledge, London.

Hugh-Hones, M. (1992). Wickham Steed and German biological warfare research. *Intell. Nat. Secur.,* **7**:379-402.

Knipe, D.M., Howley, P.M., Esposito, J.J. & Fenner, F. (2001). Poxviruses. *In:* Knipe D.M. and Howley P.M. (Eds.), *Fields Virology*. Lippincott Williams & Wilkins, Philadelphia, PA, USA, pp. 2885–2921.

Kortepeter, M.G. & Parker, G.W. (1999). Potential biological weapons threats. *Emerg. Infect. Dis.* **5**:523– 527.

Kuhn J.H., Dodd, L.E., Wahl-Jensen, V., Radoshitzky, S.R., Bavari, S. & Jahrling, P.B. (2011). Evaluation of perceived threat differences posed by filovirus variants. *Biosecur. Bioterror.* **9**:361–371.

La Placa, M. (2010). *Principles of Medical Microbiology*. Esculapio, Lahore.

Leitenberg, M. (2001). Biological weapons in twentieth century: A review and analysis. *Crit. Rev. Microbiol.*, **27**: 267-320.

Manchee, R.J., Broster, M.G., Melling, J., Henstridge, R.M. & Stagg A.J. (1981). Bacillus anthracis on Gruinard Island. *Nature,* **294**:254-255.

McCarthy, M. (2001). Anthrax attack in the USA. *Lancet Infect. Dis.* **1**:288-289.

Moquin, R.R. & Moquin, M.E. (2002). Weapons of mass destruction: biological. *Neurosurg. Focus*, **12**: E2.

Moss, B. (2007). Poxviridae: The viruses and their replication. *In:* Knipe D.M. and Howley P.M. (Eds.), *Fields Virology*. Lippincott Williams & Wilkins, Philadelphia, Pennsylvania, pp. 2905–2946.

Newark, T. (1988). *Medieval Warfare*. Bloomsbury Bools, London.

North Atlantic Treaty Organization (NATO) (1996). *NATO Handbook on the Medical Aspects of NBC Defensive Operations AMedP-6(B*). *Part II - Biological*. U.S. Department of the Army, Washington DC.

Olson, K.B. (1999). Aum Shinrikyo: Once and future threat? *Emerg. Infect. Dis.*, **5**: 513-516.

Poupard, J.A. & Miller, L.A. (1992). History of biological warfare: Catapults to capsomers. *Ann. N. Y. Aca. Sci.*, **666**: 9-20.

World Health Organization (WHO) (2004). Public Health Response to Biological and Chemical Weapons. World Health Organization (WHO), Geneva.

Rimoin, A.W., Mulembakani, P.M., Johnston, S.C., Lloyd Smith, J.O., Kisalu, N.K., Kinkela, T.L., Blumberg, S., Thomassen, H.A., Pike, B.L., Fair, J.N., Wolfe, N.D., Shongo, R.L., Graham, B.S., Formenty, P., Okitolonda, E., Hensley, L.E., Meyer, H., Wright, L.L. and Muyembe, J.J. (2010). Major increase in human monkeypox incidence 30 years after smallpox vaccination campaigns cease in the Democratic Republic of Congo. *Proc Natl Acad Sci USA,* **107**:16262–16267.

Salvato, M.S., Clegg, J.C.S., Buchmeier, M.J., Charrel, R.N., Gonzalez, J.P., Lukashevich, I.S., Peters, C.J. & Romanowski, V. (2011). Arenaviridae. *In* King, A.M.Q., Adams, M.J., Carstens, E.B., and Lefkowitz, E.J. (Eds). *Virus Taxonomy Classification and Nomenclature of Viruses: Ninth Report of the International Committee on Taxonomy of Viruses.* Elsevier-Academic Press, Oxford, pp. 715–724.

Sanchez, A., Geisbert, T.W. & Feldmann, H. (2007). Filoviridae: Marburg and Ebola Viruses. *In* Knipe D.M. and Howley P.M. (Eds.), *Fields Virology*. Lippincott Williams & Wilkins, Philadelphia, Pennsylvania, pp. 1409–48.

Schattner, M., Rivadeneyra, L., Pozner, R.G. & Gómez, R.M. (2013). Pathogenic mechanisms involved in the hematological alterations of arenavirus-induced hemorrhagic fevers. *Viruses*, **5**:340-351.

Sokolski, H.D. & James M. Ludes. (2001). *Twenty-First Century Weapons Proliferation*. Routledge, London.

Stochkholm International Peace Research Institute (SIPRI) (1971a). *The Problem of Chemical and Biological Warfare, Vol. 1: The Rise of CB Weapons*. Humanity Press. New York.

Stochkholm International Peace Research Institute (SIPRI) (1971b). *The Problem of Chemical and Biological Warfare, Vol. 2: Technical Aspects of Early Warning and Verification*. Humanity Press. New York.

Stochkholm International Peace Research Institute (SIPRI) (1973). *The Problem of Chemical and Biological Warfare, Vol. 3: CBW and the Law of War*. Humanity Press. New York.

Török, T.J., Tauxe, R.V., Wise, R.P., Livengood, J.R., Sokolow, R., Mauvais, S., Birkness, K.A., Skeels, M.R., Horan J.M. & Foster L.R. (1997). A large community outbreak of Salmonellosis caused by intentional contamination of restaurant salad bars. *JAMA*, **278**: 389-395.

Tucker, J.B. (2013). The current bioweapons threat. *In* Hunger, I., Radosavljevic, V., Belojevic, G. & Rotz, L.D. (Eds.), *Biopreparedness and Public Health*. Springer, Amsterdam, pp. 7-16.

Vela, E. (2012). Animal models, prophylaxis, and therapeutics for arenavirus infections. *Viruses,* **4**:1802-1829.

Vogel, K.M. (2012). *Phantom Menace or Looming Danger: A New Framework for Assessing Bioweapons Threats*. JHU Press, New York.

Warfield, K.L., Swenson, D.L., Demmin, G., & Bavari, S. (2005). Filovirus-like particles as vaccines and discovery tools. *Expert Rev. Vaccines*, **4**:429-440.

Weber, D.J. & Rutala, W.A. (2001). Risks and prevention of nosocomial transmission of rare zoonotic diseases. *Clin Infect Dis.*, **32**:446-456.

Weelis, M. (2002). Biological warfare at the 1346 siege of Caffa. *Emerg. Infect. Dis.,* **8**: 971-975.

World Health Organization (WHO) (2004). *Public Health Response to Biological and Chemical Weapons*. World Health Organization (WHO), Geneva, Switzerland.

World Health Organization (WHO) (2007). *WHO Guidelines on Tularaemia*. World Health Organization (WHO), Geneva, Switzerland.

Yuen, E.C.P. (2001). Biological warfare: The facts. *Hong Kong J. of Emerg. Med.* **8**:232-240.

Zalini, Y. (2010). Combating and reducing the risk of biological threats. *J. Defence Secur.*, **1**: 1-15.

EVALUATION OF THE REPEATABILITY OF GLOBAL POSITIONING SYSTEM (GPS) PERFORMANCE WITH RESPECT TO GPS SATELLITE ORBITAL PASSES

Dinesh Sathyamoorthy[*], Shalini Shafii, Zainal Fitry M Amin & Siti Zainun Ali

Instrumentation & Electronics Technology Division (BTIE), Science & Technology Research Institute for Defence (STRIDE), Ministry of Defence, Malaysia

[*]E-mail: dinesh.sathyamoorthy@stride.gov.my

ABSTRACT

This study is aimed at addressing a mistake made in the authors' previous paper on Global Positioning System (GPS) static multipath simulation (Dinesh et al., 2013), whereby it was indicated that GPS performance is repeatable for every GPS satellite orbital pass of approximately 11 h, 58 min. GPS satellites only return to the original positions with respect to the earth at every two GPS satellite orbital passes of approximately 23 h, 56 min, and hence, GPS performance is only repeatable for that period. This study demonstrates the repeatability of GPS performance with respect to GPS satellite orbital passes. It is further extended to verify the findings in Dinesh et al. (2013) in regards to GPS performance in various static multipath conditions.

Keywords: *Global Positioning System (GPS) simulation; GPS satellite orbital passes; GPS performance repeatability; estimate probable error (EPE); multipath.*

1. INTRODUCTION

In the authors' paper entitled *Evaluation of the Effect of Multipath on Global Positioning System (GPS) Performance via GPS Simulation* that was published in the Defence S&T Technical Bulletin, Vol. 6, Num. 1, pp. 62-74 (Dinesh *et al.*, 2013), it was stated that "*The repeatability of multipath at stationary sites when GPS satellites are in the same positions during each orbital pass (approximately 11 h, 58 min) allows for corrections to be generated based on history of multipath occurrences over time.*" This statement gives the impression that GPS performance is repeatable for every GPS satellite orbital pass of approximately 11 h, 58 min. However, the authors failed to take into account that the earth is rotating; when the GPS satellites complete an orbit and return to the original positions, the earth has only completed half a rotation. GPS satellites only return to the original position with respect to the earth at every two GPS satellite orbital passes of approximately 23 h, 56 min (Noordin, 2013; Humphreys, 2013; Calais, 2013). This means that

GPS performance is repeatable for approximately every 23h, 56 min, rather than every 11 h, 58 min as stated in Dinesh *et al.* (2013).
It should be noted the study in Dinesh *et al.* (2013) was conducted for a period of 9 h (17 February 2013, UTC 000-0900). Hence, the findings in the paper with respect to GPS performance in various static multipath conditions still stand. The only mistake made in this paper was that the authors misunderstood the orbital passes of GPS satellites with respect to the earth, with no follow up tests conducted to verify it.

This study is aimed at evaluating the repeatability of GPS performance with respect to GPS satellite orbital passes. It will be conducted using GPS simulation, which will allow the tests to be held with various repeatable conditions, as defined by the authors. As the tests are conducted in controlled laboratory environments, they will not be inhibited by unintended signal interferences and obstructions (Aloi *et al.*, 2007; Dinesh *et al.*, 2009; Petrovski *et al.*, 2010; Kou & Zhang 2011; Pozzobon *et al.*, 2013). GPS simulation was previously used to study the vulnerabilities of GPS to radio frequency interference (RFI) in Dinesh *et al.* (2012a, b) and multipath in, the paper that is the bone of contention for this study, Dinesh *et al.* (2013). The study will be further extended to verify the findings in Dinesh *et al.* (2013) on GPS performance in various static multipath conditions.

2. METHODOLOGY

The apparatus used in the study are an Aeroflex GPSG-1000 GPS simulator (Aeroflex, 2010), a notebook running GPS Diagnostics v1.05 (CNET, 2004), and a Garmin GPSmap 60CSx handheld GPS receiver (Garmin, 2007), which employs the GPS L1 coarse acquisition (C/A) signal. The study is conducted in STRIDE's mini-anechoic chamber (Kamarulzaman, 2010) to avoid external interference signals and unintended multipath errors. The test setup employed is as shown in Figure 1. Simulated GPS signals are generated using the GPS simulator and transmitted via the coupler. The following assumptions are made for the tests conducted:

i. No ionospheric or troposheric delays
ii. Zero clock and ephemeris error
iii. No unintended obstructions or multipath
iv. No interference signals.

The tests are conducted for 1 h intervals for every 6 h starting from 18 June 2013, UTC 0000 to 21 June 2013, UTC 1800. The almanac data for the periods is downloaded from the US Coast Guard's web site (USCG, 2013), and imported into the GPS simulator. The GPS signal power level is set at -130 dBm, while the coordinates are set at N 2° 58' E 101° 48' (Kajang, Selangor).

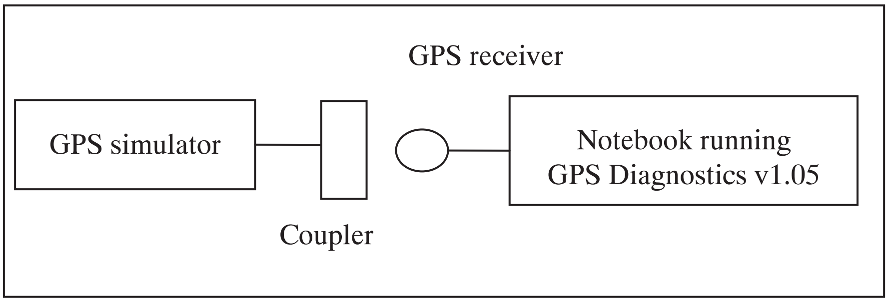

Figure 1: The test setup employed.

Multipath refers to the distortion of direct line-of-sight (LOS) Global Navigation Satellite System (GNSS) signals by localised reflected / diffracted signals, caused by objects such as trees, buildings, etc. As the multipath signals travel additional distances, they are delayed relative to the LOS signals, resulting in range measurements to the GNSS satellites being severely degraded. The multipath signals' paths are dependent on the reflecting surfaces and satellites' positions. As the satellites move with time, the multipath effect is also a variable of time. Multipath error is dependent on the architecture of GNSS receivers, in terms of the different ways the receivers deal with the signals (Gerdan *et al.*, 1995; Weill, 1997; Hannah, 2001; Kos *et al.*, 2010; Mekik & Can, 2010; Matsushita & Tanaka, 2012).

As with Dinesh *et al.,* 2013, multipath simulations in this study are conducted based on important characteristics of GPS signal obstruction and multipath (Gerdan *et al.*, 1995; Weill, 1997; Hannah, 2001; Kos *et al.*, 2010; Mekik & Can, 2010; Matsushita & Tanaka, 2012):

i) Physical obstructions prevent certain GPS signals from reaching the GPS receiver, causing a reduction in number of visible GPS satellites
ii) Multipath signals that are reflected off physical obstructions have lower power levels as compared to unaffected GPS signals
iii) The effects of GPS signal obstruction and multipath can be correlated with GPS satellite elevation, with the effects being at a maximum during low elevations and improving for higher elevations.

As indicated in Dinesh *et al.*, 2013, the GPS simulator does not provide specific multipath simulation. However, it does allow for selection of GPS satellites and signal power levels. Based on this, the study is conducted by assuming various conditions of physical obstructions and multipath signals (Table 1). It is assumed that each multipath signal undergoes a reduction in power level of 15 dBm. Readings are taken for periods of 15 min (the maximum viable period for the assumptions made in Table 1) on 18-21 June 2013 at UTC times of 0000, 0600, 1200 and 1800.

Table 1: Test scenarios used for the study.
(Source: Dinesh *et al.*,2013)

Reading	Scenario	Number of Visible Satellites	Number of Multipath Signals
1	No physical obstructions or multipath, and hence, the full range of visible satellites are available.	8-10	0
2	Physical obstructions result in only four GPS satellites, with the highest elevations, being visible, but multipath does not occur.	4	0
3	Physical obstructions result in only four GPS satellites, with the highest elevations, being visible. Of the four available GPS signals, the signal from the satellite with the lowest elevation undergoes multipath.	4	1
4	Physical obstructions result in only four GPS satellites, with the highest elevations, being visible. Of the four available GPS signals, two signals from the satellites with the lowest elevations undergo multipath.	4	2
5	Physical obstructions result in only four GPS satellites, with the highest elevations, being visible. Of the four available GPS signals, three signals from the satellites with the lowest elevations undergo multipath.	4	3
6	Physical obstructions result in only four GPS satellites, with the highest elevations, being visible, with all the signals undergoing multipath.	4	4

3. RESULTS & DISCUSSION

Trimble Planning (Trimble, 2013) is used to estimate GPS satellite coverage at the test area for the periods of the study in terms of position dilution of precision (PDOP) (Figure 2), which represents the effect of GPS satellite geometry on 3D positioning precision. A PDOP value of 1 is associated with an ideal arrangement of the satellite constellation. To ensure high-precision GPS positioning, a PDOP value of 5 or less is usually recommended. In practice, the actual PDOP value is usually much less than 5, with a typical average value in the neighbourhood of 2 (DOD, 2001; USACE, 2011; Kaplan & Hegarty, 2006; Huihui *et al.*, 2008; Dinesh *et al.*, 2010). It is observed that the PDOP profiles for all four days are similar, with the profile for each day shifted by approximately 4 min earlier from the previous day, corresponding to the difference between an earth day (24 h) and two GPS satellite orbital passes (23 h, 56 min).

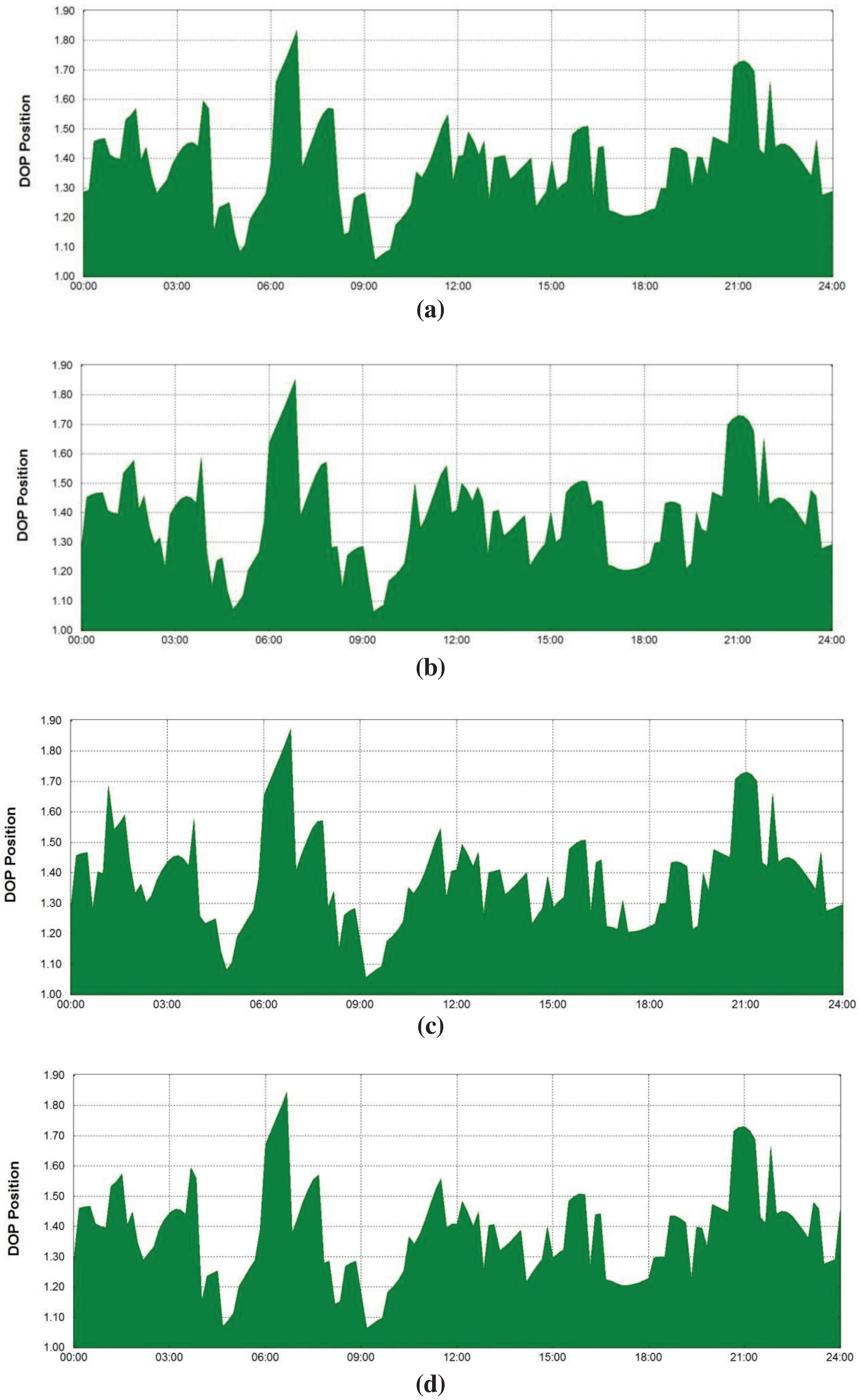

Figure 2: PDOP of GPS coverage at the test area for simulation dates of (a) 18, (b) 19, (c) 20 and (d) 21 June 2013.
(Source: Screen captures from Trimble Planning)

The estimate probable error (EPE) values recorded for the readings are shown in Figure 3. EPE provides a 3D confidence ellipsoid that depicts uncertainties of GPS location fixes. It is computed by multipying PDOP with user equivalent ranging error (UERE), which is the total expected magnitude of position errors due to measurement uncertainties from the various error components for a particular GPS receiver (DOD, 2001; USACE, 2011; Kaplan & Hegarty, 2006). As with the PDOP profiles in Figure 2, the EPE profiles for all four days are similar, with the profile for each day shifted by approximately 4 min earlier from the previous day.

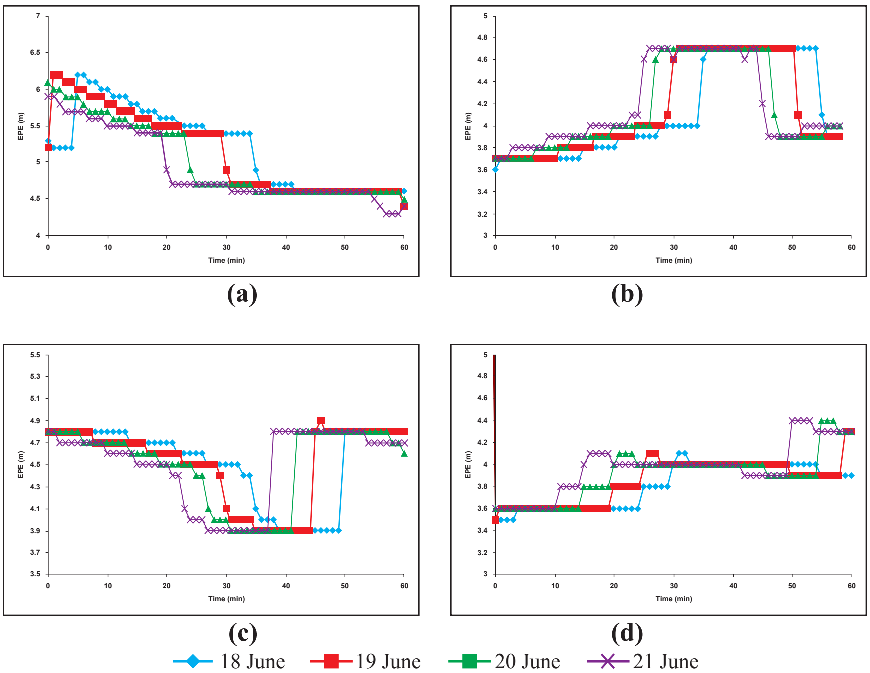

Figure 3: Recorded EPE values for UTC times of (a) 0000, (b) 0600, (c) 1200 and (d) 1800.

The recorded EPE values for the multipath simulations are shown in Figures 4-7. As indicated in Dinesh *et al.* (2013), the decrease in number of visible satellites due to physical obsructions and increase in number of multipath signals caused increase in EPE values. This is due to decreasing carrier-to-noise density (C/N_0) levels for GPS satellites tracked by the receiver, which is the ratio of received GPS signal power level to noise density. Lower C/N_0 levels result in increased data bit error rate when extracting navigation data from GPS signals, and hence, increased carrier and code tracking loop jitter. This, in turn, results in more noisy range measurements and thus, less precise positioning (DOD, 2001; USACE, 2011; Kaplan & Hegarty, 2006; Petovello, 2009). The tests conducted in this study employed GPS signal power level of-130 dBm. Usage of lower GPS signal power levels would result in reduced C/N_0 levels and hence, higher rates of increase of EPE values.

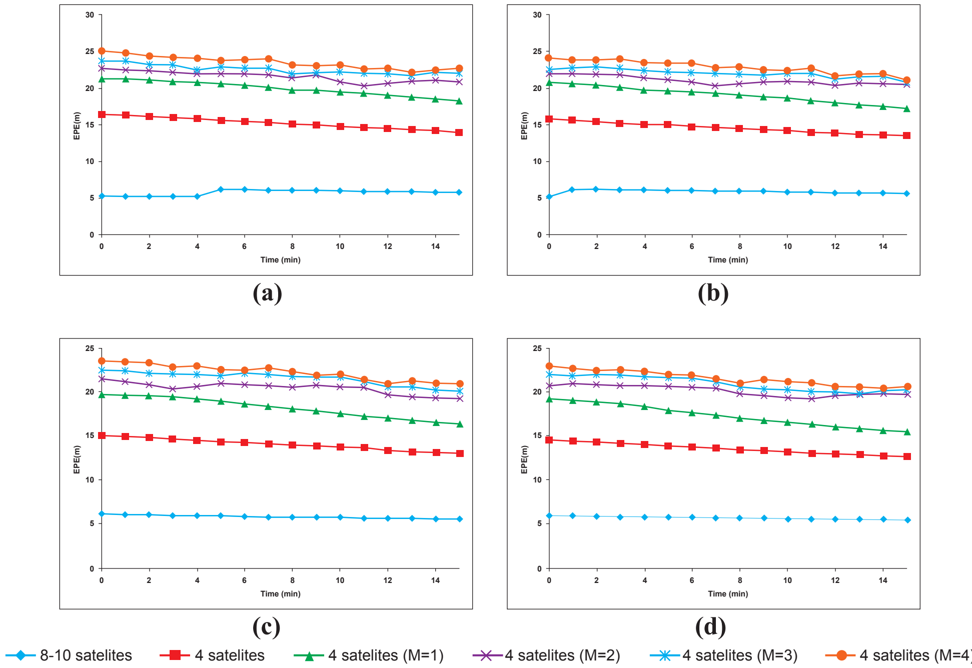

Figure 4: Recorded EPE values for multipath simulations at UTC 0000 on (a) 18, (b) 19, (c) 20 and (d) 21 June 2013. *M* is the number of multipath signals.

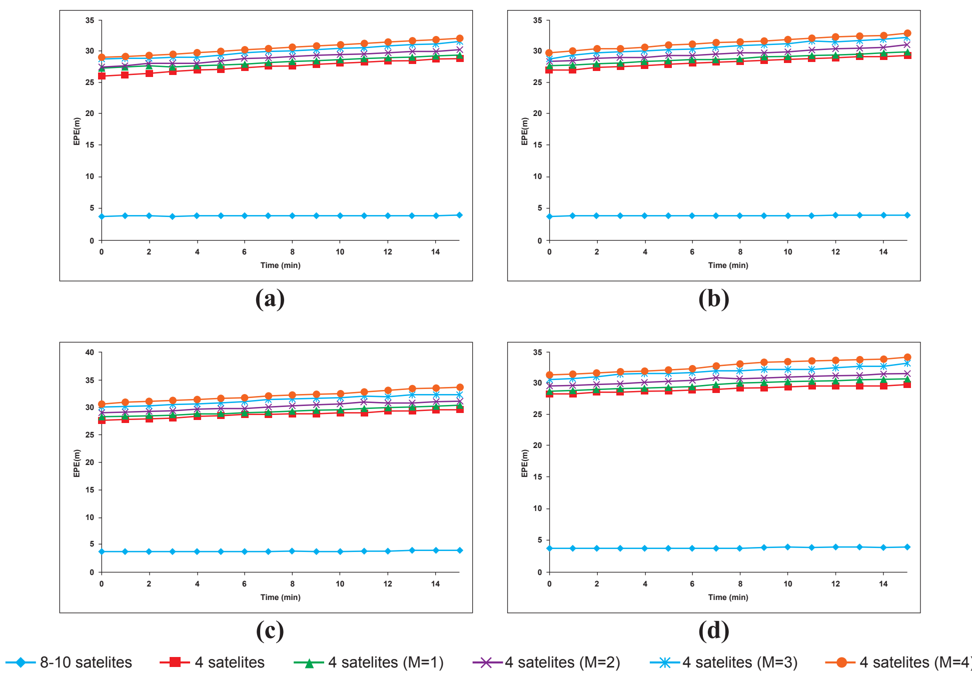

Figure 5: Recorded EPE values for multipath simulations at UTC 0600 on (a) 18, (b) 19, (c) 20 and (d) 21 June 2013. *M* is the number of multipath signals.

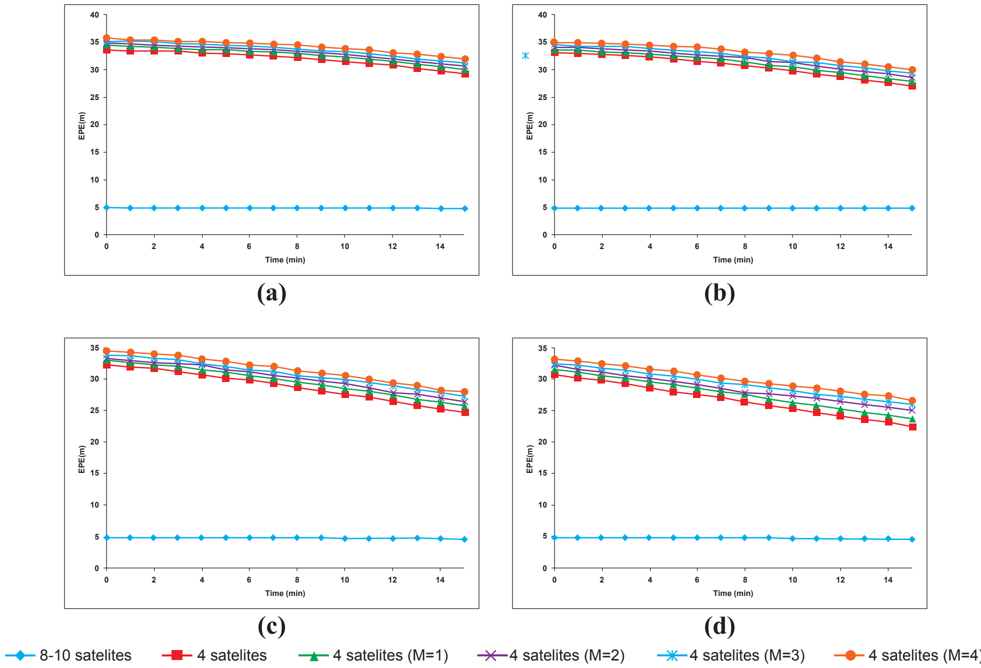

Figure 6: Recorded EPE values for multipath simulations at UTC 1200 on (a) 18, (b) 19, (c) 20 and (d) 21 June 2013. *M* is the number of multipath signals.

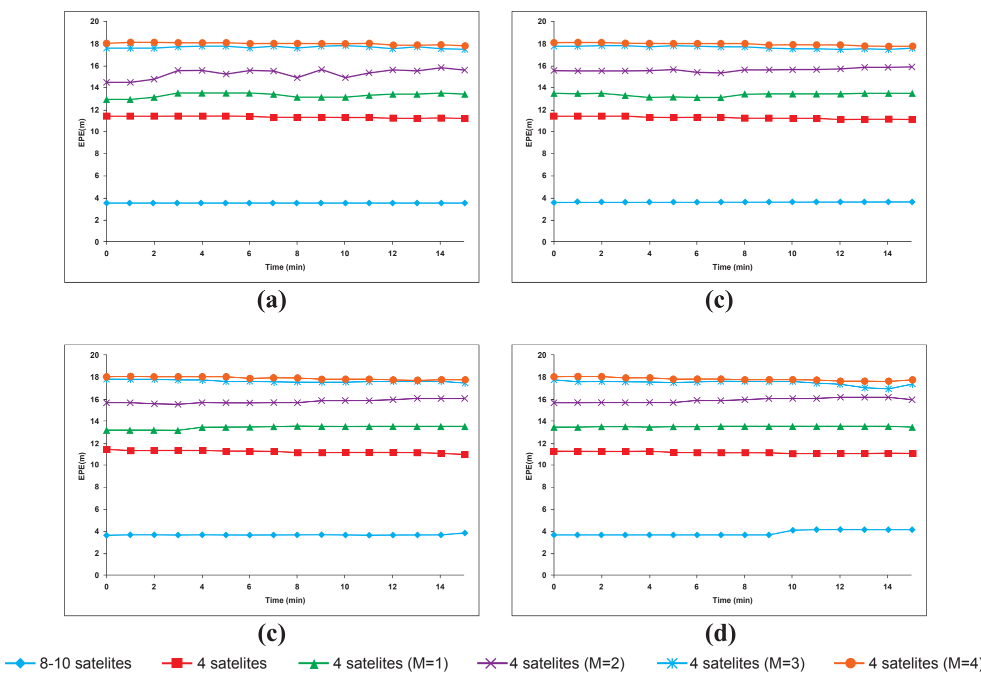

Figure 7: Recorded EPE values for multipath simulations at UTC 1800 on (a) 18, (b) 19, (c) 20 and (d) 21 June 2013. *M* is the number of multipath signals.

Varying probable error patterns are observed for readings taken at different times. This is due to the GPS satellite constellation being dynamic, causing varying GPS satellite geometry over time, resulting in GPS accuracy being time dependent (DOD, 2001; USACE, 2011; Kaplan & Hegarty, 2006; Huihui *et al.*, 2008; Dinesh *et al.*, 2010). Multipath is highly repeatable as it is approximately the same when the GPS satellites are in the same positions with respect to the earth at every two orbital passes (approximately 23 h, 56 min). This repeatability can be used to build a history of multipath occurrences over time, which can then be used to generate multipath corrections for stationary sites.

4. CONCLUSION

This study has demonstrated the repeatability of GPS performance when GPS satellites are in the same positions with respect to the earth for every two GPS satellite orbital passes of 23 h, 56 min. In addition, the findings in Dinesh *et al.* (2013) in regards to GPS performance in various static multipath conditions were also verified. On the whole, the findings of this study demonstrate that the repeatability of GPS performance at stationary sites can be used to generate multipath corrections based on history of multipath occurrences over time.

ACKNOWLEDGEMENT

The authors would like to apologise to the editorial board of the Defence S&T Technical Bulletin for the mistake that was made in Dinesh *et al.* (2013) in regards to orbital passes of GPS satellites with respect to the earth. We are grateful to Dr. Noordin Ahmad, Deputy Director-General of the National Space Agency, Malaysia, and Asst. Prof. Dr. Todd Humphreys, Department of Aerospace Engineering and Engineering Mechanics, University of Texas at Austin, US, for their suggestions that have helped strengthen this manuscript.

REFERENCES

Aeroflex (2010). *Avionics GPSG-1000 GPS / Galileo Portable Positional Simulator*. Aeroflex Inc., Plainview, New York.

Aloi, D.N., Alsliety, M. & Akos, D.M. (2011). A methodology for the evaluation of a GPS receiver performance in telematics applications. *IEEE T. Instrum. Meas.*, **56**: 11-24.

Calais, E. (2013). *Satellite Orbits*. Purdue University, West Lafayette, Indiana.

CNET (2004). *GPSDiag 1.0*. Available online at: http://download.cnet.com/GPSDiag/3000-2130_4-4951103.html (Last access date: 31 January 2010).

Department of Defence (DOD) (2001). *Global Positioning System Standard Positioning Service Performance Standard*. Command, Control, Communications, And Intelligence, Department of Defence (DOD), Washington D.C.

Dinesh , S., Wan Mustafa, W.H., Mohd Faudzi., M., Kamarulzaman, M., Nor Irza Shakhira, B., Siti Robiah, A., Norhayaty, Z., Aliah, I., Lim, B.T., Arumugam, P., Zainal Fitry, M.A., Mohd. Rizal, A.K., Azlina, B. & Mohd. Hasrol, H.M.Y. (2009). The advantages of Global Navigation Satellite Systems (GNSS) receiver evaluation using GNSS simulators. *BUDI*, **2009**: 6-10.

Dinesh , S., Wan Mustafa, W.H., Mohd Faudzi., M., Kamarulzaman, M., Hasniza, H., Nor Irza Shakhira, B., Siti Robiah, A., Shalini, S., Jamilah, J., Aliah, I., Lim, B.T., Zainal Fitry, M.A., Mohd. Rizal, A.K., Azlina, B. & Mohd. Hasrol, H.M.Y. (2010). Evaluation of the effect of radio frequency interference (RFI) on Global Positioning System (GPS) accuracy. *Defence S&T Tech. Bull.*, **3**: 100-118.

Dinesh, S., Mohd Faudzi., M., Rafidah, M., Nor Irza Shakhira, B., Siti Robiah, A., Shalini, S., Aliah, I., Lim, B.T., Zainal Fitry, M.A., Mohd. Rizal, A.K., & Mohd Hasrol, H.M.Y. (2012a). Evaluation of the effect of radio frequency interference (RFI) on the Global Positioning System (GPS) L1 coarse acquisition (C/A) signal via GPS simulation. *11th International Symposium & Exhibition on Geoinformation 2012 (ISG2012)*, 25-26 September 2012, Hotel Istana Kuala Lumpur City Centre, Kuala Lumpur.

Dinesh, S., Mohd Faudzi., M. & Zainal Fitry, M.A. (2012b). Evaluation of the effect of radio frequency interference (RFI) on Global Positioning System (GPS) accuracy via GPS simulation. *Defence Sci. J.*, **62**: 338-347.

Dinesh, S., Shalini, S., Zainal Fitry, M.A. & Siti Zainun, A. (2013). Evaluation of the effect of multipath on Global Positioning System (GPS) performance via GPS simulation. *Defence S&T Tech. Bull.*, **6**: 62-74.

Garmin (2007). *GPSmap 60CSx Owner's Manual*. Garmin International Inc., Olathe, Kansas.

Gerdan, G.P., Coombe, L.J. & Takac, F. (1995). *The Effects of RF Interference, Multipath and Signal Obstruction on the GPS Observables*. Department of Land Information, Royal Melbourne Institute of Technology (RMIT), Melbourne, Victoria.

Hannah, B. (2001). *Modelling and Simulation of GPS Multipath Propagation*. PhD Dissertation, Queensland University of Technology, Brisbane, Queensland.

Huihui, W., Xingqun, Z. & Yanhua, Z. (2008). Geometric dilution of precision for GPS single-point positioning based on four satellites. *J. Syst. Eng. Electr.*, **19**: 1058-1063.

Humphreys. T. (2013). Personal communication with Asst. Prof. Dr. Todd Humphreys, Department of Aerospace Engineering and Engineering Mechanics, University of Texas at Austin, US.

Kaplan, E.D. & Hegarty, C.J. (2006). *Understanding GPS: Principles and Applications*. Artech House, Norwood, Massachusetts.

Kamarulzaman, M. (2010). *Technical Specification for STRIDE's Mini-Anechoic Chamber*. Science & Technology Research Institute for Defence (STRIDE), Ministry of Defence, Malaysia.

Kos, T., Markezic, I. & Pokrajcic, J. (2010). Effects of multipath reception on GPS positioning performance. *52nd International Symposium ELMAR-2010*, 15-17 September 2010, Zadar, Croatia.

Kou, Y. & Zhang, H. (2011). Verification testing of a multi-GNSS RF signal Simulator. *Inside GNSS*, **6**: 52-61.

Matsushita, T. & Tanaka, T. (2012). Study on improving the accuracy of satellite measurement in urban areas. *T. Soc. Instrumen. Control Eng.*, **48**: 73-77.

Mekik, C. & Can. O. (2010). Multipath effects on RTK GPS and a case study. *2010 International Symposium on GPS / GNSS*, 26-28 October 2010, Taipei, Taiwan.

Noordin, A. (2013). Personal communication with Dr. Noordin Ahmad, Deputy Director-General of the National Space Agency, Malaysia.

Petovello, M. (2009). Carrier-to-noise density and AI for INS / GPS integration. *Inside GNSS*, **4**: 20-29.

Petrovski, I., Townsend, B. & Ebinuma, T. (2010). Testing multi-GNSS equipment: Systems, simulators and the production pyramid. *Inside GNSS*, **5**: 52-61.

Pozzobon, O., Sarto, C., Chiara, A.D., Pozzobon, A., Gamba, G., Crisci, M. & Ioannides, R. (2013). Developing a GNSS position and timing authentication testbed: GNSS vulnerability and mitigation techniques. *Inside GNSS*, **8**: 45-53.

Trimble (2013). *Trimble's Planning Software*. Available online at:

http://www.trimble.com/planningsoftware.shtml (Last access date: 21 February 2013).

US Army Corps of Engineers (USACE) (2011). *Engineer Manual EM 1110-1-1003: NAVSTAR Global Positioning System Surveying.* US Army Corps of Engineers (USACE), Washington D.C.

US Coast Guard (USCG) (2013). *GPS NANUs, Almanacs, & Ops Advisories*. Available online at:

http://www.navcen.uscg.gov/?pageName=gpsAlmanacs (Last access date: 22 July 2013).

Weill, L.R. (1997). Conquering multipath: The GPS accuracy battle. *GPS World*, **April 1997**: 59-66.